

Molecularly Stimuli-Responsive Self-Assembled Peptide Nanoparticles for Targeted Imaging and Therapy

Yang Zhou,[#] Qianqian Li,[#] Ye Wu, Xinyu Li, Ya Zhou, Zhu Wang, Hui Liang, Feiqing Ding, Sheng Hong, Nicole F. Steinmetz,* and Hui Cai*



Cite This: <https://doi.org/10.1021/acsnano.3c01452>



Read Online

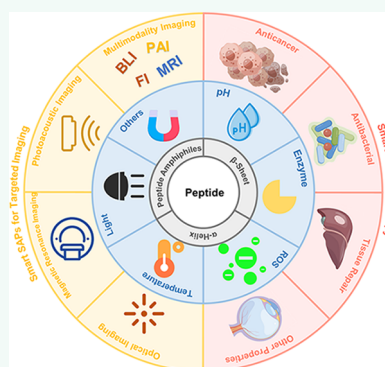
ACCESS |

Metrics & More

Article Recommendations

ABSTRACT: Self-assembly has emerged as an extensively used method for constructing biomaterials with sizes ranging from nanometers to micrometers. Peptides have been extensively investigated for self-assembly. They are widely applied owing to their desirable biocompatibility, biodegradability, and tunable architecture. The development of peptide-based nanoparticles often requires complex synthetic processes involving chemical modification and supramolecular self-assembly. Stimuli-responsive peptide nanoparticles, also termed “smart” nanoparticles, capable of conformational and chemical changes in response to stimuli, have emerged as a class of promising materials. These smart nanoparticles find a diverse range of biomedical applications, including drug delivery, diagnostics, and biosensors. Stimuli-responsive systems include external stimuli (such as light, temperature, ultrasound, and magnetic fields) and internal stimuli (such as pH, redox environment, salt concentration, and biomarkers), facilitating the generation of a library of self-assembled biomaterials for biomedical imaging and therapy. Thus, in this review, we mainly focus on peptide-based nanoparticles built by self-assembly strategy and systematically discuss their mechanisms in response to various stimuli. Furthermore, we summarize the diverse range of biomedical applications of peptide-based nanomaterials, including diagnosis and therapy, to demonstrate their potential for medical translation.

KEYWORDS: *self-assembled peptide, nanoparticle, stimuli-responsive, peptide nanoparticle, biomaterials, biomedical therapy, bioimaging diagnosis, peptide-based nanomaterials*



Orthogonal self-assembly is a ubiquitous and vital process for constructing a living cell, starting with the cytoskeleton and mediating signal pathways.¹ Dysregulated self-assembly processes are the underlying cause for diseases, such as amyloid protein deposits in neurodegenerative diseases.² Nature-inspired self-assembled materials build ordered architectures that are ideal for biomedical applications. Among them, self-assembled peptides (SAPs), “bottom-to-up” built up by amino acids, have been widely utilized owing to their structural programmability, good biocompatibility, low immunogenicity, and versatile functionality.³ Peptides could function as building blocks,⁴ targeting motifs,⁵ therapeutic reagents,⁶ and adhesion materials,⁷ thus providing versatile biomedical applications, such as drug delivery,⁸ tissue repair,⁹ and imaging.¹⁰

Molecularly stimuli-responsive SAP nanoparticles, termed “smart” nanoparticles, have recently emerged for precise biological applications. These SAP nanoparticles use differences in the pathophysiological microenvironment (internal

stimuli such as pH, enzymes, and membrane receptors) between the lesion area and healthy tissue or rely on external stimuli (light, temperature, ultrasound, and magnetic fields) to trigger self-assembly.¹⁰ Mechanistically, stimuli-responsive SAPs are capable to cleave labile or responsive bonds or change peptide properties, such as surface charge, to regulate self-assembly behaviors, further achieving on demand biomedical application, for example, enzyme-instructed self-assembly (EISA) using an enzyme-specific recognition site to manipulate the self-assembly process.¹¹ Compared to other materials, diverse biomedical applications can be precisely

Received: February 14, 2023

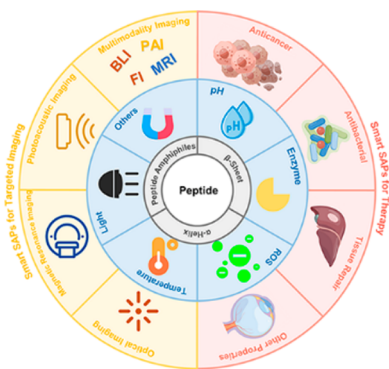
Accepted: April 17, 2023

Published: April 20, 2023

realized by SAP nanoparticles based on reasonable design of morphological transformations upon indicated conditions with good biocompatibility.¹²⁻¹⁸ When functioning as a delivery carrier, molecularly stimuli-responsive SAPs bind to the cargo through electrostatic, $\pi-\pi$ stacking, or hydrophobic interactions to prevent drug leakage and degradation and achieve controlled release by stimuli for drug accumulation at pathological tissue.¹⁹ As bioimaging agents, *in situ* morphological transformation or self-assembly enables smart localization and enrichment of imaging agents at the target sites for improving signal-to-noise ratio.²⁰ Moreover, targeted imaging combined with therapy allows for longitudinal imaging and ad-hoc adjustment of therapy thus improving outcomes.²¹ As an anticancer strategy, molecularly stimuli-responsive SAPs could function as anticancer agents themselves and aggregate around malignant cells upon stimuli to prevent tumor material change and metastasis.²² Based on their designable conformation change and composable function modules, molecularly stimuli-responsive SAPs have been widely used in biomedicine as antitumor, antibacterial, tissue repair, and imaging agents, among other uses.²³

This review demonstrates the self-assembly mechanism of SAPs and summarizes the smart design of SAPs in response to external/internal stimuli reported in recent years as well as their advantages and the challenges they are facing for targeted imaging and therapy ([Scheme 1](#)). This review may provide a reference for developing SAPs-based medical products and further promote the clinical transformation of these nano-systems.

Scheme 1. Schematic Illustration of Molecularly Stimuli-Responsive Self-Assembled Peptides (Smart SAPs) including Driving Forces, Regulatory Stimuli, and Biomedical Applications



MECHANISMS OF SELF-ASSEMBLED BEHAVIOR

Peptide self-assembly is driven by the instability of monomers in aqueous conditions. Intramolecular folding of monomer exhibited insufficient hydrophilic surface to form a protective hydration layer. The polymerization process allows intermolecular assembly to produce higher hierarchical aggregates with lower free energy, with hydrophobic residues well-assembled in the core and hydrophilic groups directed toward the solution. The mechanisms that drive the self-assembly performance of peptides mainly include β -sheet mediated self-assembly, α -helix mediated self-assembly, and amphiphilic feature mediated self-assembly.

β -Sheet Mediated Self-Assembly. β -Sheets are the most common motifs extensively utilized in promoting peptide self-assembly. β -Sheet folding depends on the hydrogen bonds between amides in the framework of two adjacent β -strands. In most cases, residues in the side chains of polypeptides contribute to the formation and stability of β -sheets through additional electrostatic interactions or $\pi-\pi$ stacking. Moreover, the assembly of β -sheets results in more complicated and hierarchical structures.

Q11 (Ac-QQKFQFQFEQQ-Am), a well-established β -sheet-forming peptide (Figure 1A), is designed to maximally

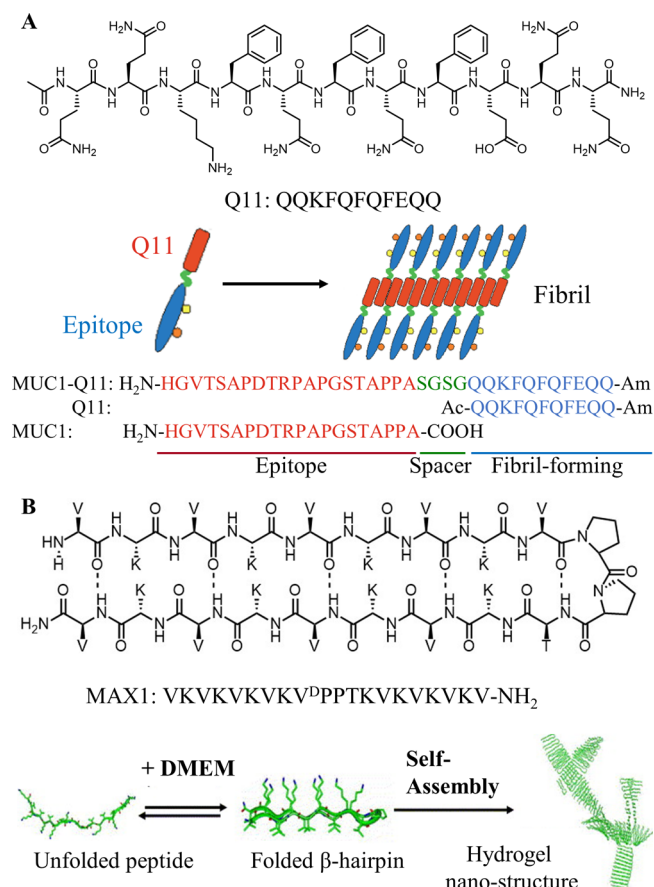


Figure 1. Schematic illustration of β -sheet mediated self-assembly. (A) Peptide Q11 with β -sheet structure used as the scaffold to construct self-assembling, adjuvant-free MUC1 glycopeptide vaccines. Adapted with permission from ref 25. Copyright 2012 American Chemical Society. (B) Peptide MAX1 folded to an amphiphilic β -hairpin and self-assembled into hydrogel nanostructure stimulated by DMEM cell culture media. Adapted with permission from ref 29. Copyright 2002 American Chemical Society. Adapted with permission from ref 30. Copyright 2005 Elsevier Ltd.

utilize the interaction between the side chains of the β -strands. The amide group of glutamine (Q) forms hydrogen bonds. The primary amine of lysine (K) and the carboxyl group of glutamate (E) interact via electrostatic interactions. The benzyl group between two phenylalanines (F) forms $\pi-\pi$ stacking. Therefore, Q11 tends to be an unbranched antiparallel β -sheet. The presence of functional groups or bioactive peptides at the Q11 terminus and the tuning of side residues endow Q11 with versatile environmental responsiveness and diverse applications. For example, β -sheet-forming peptides function as

scaffolds to display immunogenic epitopes in vaccines for peptide-based immunotherapies.²⁴ Q11 has been conjugated with MUC1 glycopeptides to construct self-assembling, adjuvant-free MUC1 glycopeptide vaccines for cancer therapy.²⁵

In aqueous media, peptides comprising alternating hydrophilic and hydrophobic residues tend to form β -sheet structures with a hydrophobic face on one side and hydrophilic on the other. They form β -sheet bilayers through parallel or antiparallel alignment and further form fibrils through intra- and intermolecular hydrogen bonds and/or electrostatic interactions. In addition to nanofibers, other hierarchical structural arrays, including ribbons, tapes, and fibrils, can also be designed.²⁶ The classical example in nature is the self-assembling peptide (AEAEAKAK)₂-CONH₂ found in the yeast protein Zuoitin.²⁷ Moreover, the aggregation of dipeptide repeats, such as (GR)_n and (PR)_n, translated from hexanucleotide repeat expansion C9orf72, was considered a potential mechanism of amyotrophic lateral sclerosis (ALS) and frontotemporal dementia (FTD).²⁸ MAX1, a 20 amino acid peptide that can fold and form an amphiphilic β -hairpin, is designed based on this principle (Figure 1B).²⁹ The MAX1 sequence (NH₂-VKVKVKVK^DPPTKVKVKVK-CONH₂) comprises alternating lysine and valine residues on two β -strands that flank a type II' β -turn.³⁰ Peptide folding is directly related to self-assembly. Therefore, the conditions that facilitate hairpin formation will also facilitate hydrogel formation.³⁰

In addition to Q11 and MAX1, numerous peptides have been designed to form β -sheets. For instance, Phe-Phe (FF) or certain FF-containing peptides directly form β -sheet aggregates and spontaneously self-assemble into nanotubes through π - π stacking in aqueous solutions, which can be widely applied in optics, energy storage/conversion, and healthcare.³¹ β -Sheet-forming peptides highly occur in neurodegenerative diseases, such as polyQ-decorated huntingtin in Huntington's, $\text{A}\beta$ in Alzheimer's, and α -synuclein in Parkinson's disease.³²⁻³⁴ The β -sheet-forming peptide designed for biomedicine application should be orthogonal to naturally existing β -sheet-forming peptides or proteins to avoid chronic aggregation of endogenous peptides or proteins.

α -Helix Mediated Self-Assembly. α -Helices are formed by hydrogen bonds between the main-chain amides with a 3.6 residue distance. Interaction with other α -helices is possible through the side chains of the amino acids protruding from the helix. Coiled-coil (CC) structures are formed through the assembly of α -helices into higher-order structures called hydrogelating self-assembling fibers (hSAF).^{26,35} Generally, leucine zippers and coiled-coil proteins have a 7-residue repeat of hydrophobic (H) and polar (P) residues, (HPPHPPP)_n, labeled a-g (Figure 2A), which guides the folding and subsequent assembly of amphipathic α -helices to form the so-called CC. Collagen naturally aggregates into hSAF through the CC structures. Inspired by the collagen protein structure and function, the Pro-Phe-Phe peptide, derived from collagen, forms helical-like sheets that mate via hydrophobic aromatic interfaces. Furthermore, reengineering Pro-Phe-Phe by substituting proline with hydroxyproline (Hyp), an essential collagen component, affords a superhelical assembly with mechanical rigidity comparable to that of collagen fibers.³⁶

Two 28-residue self-assembling fiber peptides, SAF-p1 and SAF-p2, can be mixed to fold and form extended coiled-coil fibers.³⁷ SAF-p1 and SAF-p2 comprise two complementary

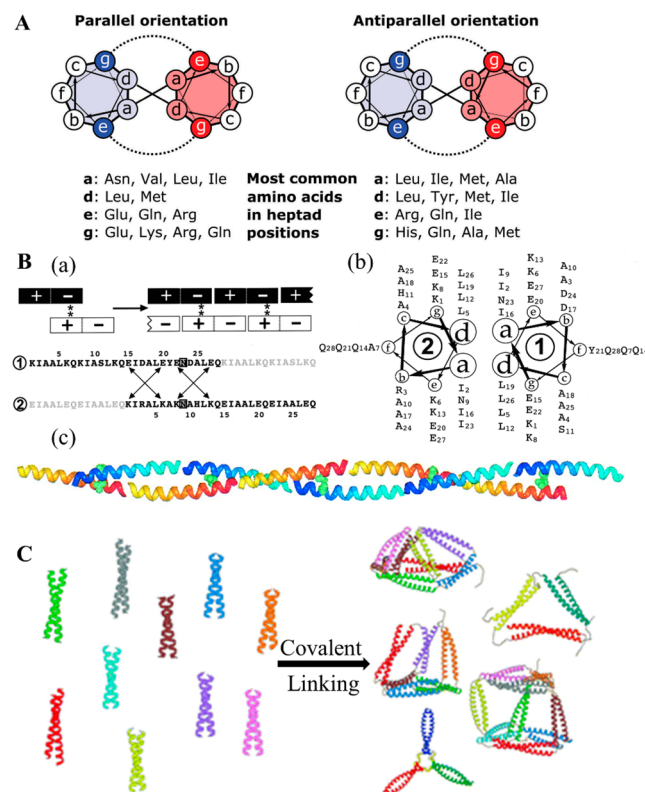


Figure 2. Schematic illustration of α -helix mediated self-assembly.
(A) Coiled-coil structure is formed through the assembly of α -helices. Adapted with permission under a Creative Commons Attribution 3.0 Unported License from ref 35. Copyright 2018 Royal Society of Chemistry. **(B)** Diagram of the designed self-assembling fiber. (a) A sticky-end assembly process and the sequences of the self-assembling fiber (SAF) peptides. Circled numbers indicate related peptide numbers, asterisks indicate asparagine residues, and arrows indicate complementary electrostatic interactions. (b) Helical-wheel formed by SAF peptides. **(c)** Diagram of the designed self-assembling fiber. SAF-p1 (colored yellow-to-red from the N- to the C-terminus) and SAF-p2 (colored blue-to-cyan from the N- to the C-terminus) form extended coiled-coil fibers when mixed. Adapted with permission from ref 37. Copyright 2000 American Chemical Society. **(C)** The coiled-coil protein origami (CCPOs) strategy can lead to the successful *de novo* design of protein cages in the shape of a tetrahedron, square pyramid and triangular prism. Adapted with permission under a Creative Commons Attribution 3.0 Unported License from ref 35. Copyright 2018 Royal Society of Chemistry.

leucine-zipper peptides co-assembled into sticky-ended heterodimers with complementary overhanging ends, which promote the formation of long fibers (Figure 2B).

To further stabilize lateral fiber assembly in the SAFs, Woolfson et al.³⁸ enhanced potentially complementary features that presented on the surface of the leucine-zipper building blocks of the SAF-p1/SAF-p2 design. They redesigned SAF-p2 by incorporating two arginine residues at two consecutive c sites. This constructed peptide, SAF-p2a, should combine with SAF-p1 to form protofibrils with matching acidic and basic patches on their surfaces. This rational redesign led to thicker and more stable second-generation fibers.

Based on the self-assembly mechanism of hSAF, CC peptide modules represent an important modular design principle that drives the design of coiled-coil protein origamis (CCPOs) (Figure 2C). CCPOs are based on multiple CC modules

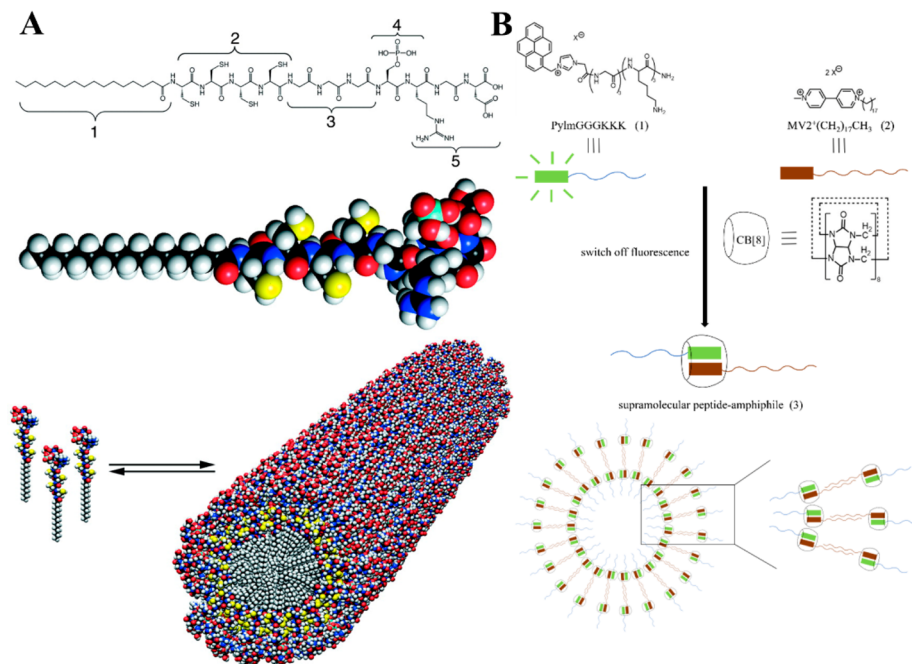


Figure 3. Schematic illustration of amphiphilic feature mediated self-assembly. (A) A single tail lipidated PA including five different structural elements. Adapted with permission from ref 41. Copyright 2001 The American Association for the Advancement of Science. (B) A vesicle constructed by a supramolecular PA. Inside the CB[8] cavity, a pyrene modified short hydrophilic peptide and a viologen labeled lipid were inserted simultaneously and were responsive to a variety of external triggers. Adapted with permission from ref 43. Copyright 2012 Wiley-VCH Verlag GmbH & Co. KGaA, Weinheim.

concatenated into a single polypeptide chain. When peptide segments assemble into CC dimers, the resulting polypeptide chain folds into a polyhedral protein cage. Designing versatile CCPOs requires the availability of orthogonal building modules, a peptide collection that assembles into CCs only with their predetermined partners. Jerala et al.³⁵ summarized the successful designs of protein nanostructures using orthogonal CC sets with an emphasis on CCPO structures and potential applications. The CCPO strategy has led to the successful *de novo* design of tetrahedron, square pyramid, or triangular prism protein cages. For instance, Woolfson et al.³⁹ engineered two CC modules: a shorter (~20 residues) homotrimer and a similarly short obligate heterodimer comprising acidic and basic residues joined consecutively to render two complementary hubs and form hexagonal networks that close to form cages when mixed.

Amphiphilic Feature Mediated Self-Assembly. PAs can be categorized into (1) amphiphilic peptides, composed of amino acids only; (2) lipidated PAs, with lipid groups attached to the C-terminal or N-terminal of peptides; and (3) supramolecular PA conjugates.⁴⁰ PA aggregation is mainly driven by hydrophobic and hydrophilic interactions. Simultaneously, the peptide segments have the potential to form diverse secondary structures, which further contribute to the stability of the fibers.

PAs comprising repetitive dyads of hydrophobic and hydrophilic residues often adopt β -sheet-like structures, as summarized in the *β -Sheet Mediated Self-Assembly* section. Herein, we primarily introduce lipidated PAs. A single-tail lipidated PA was reported by Stupp et al.,⁴¹ which contained five different structural elements (Figure 3A). The first element was a hydrophobic palmitoyl group at the N-terminus connected to the second element, comprising four cysteine residues, which provided an oxidative polymerization site. The

third element was a flexible linker of three glycine residues, linked with the fourth element, phosphorylated serine-containing peptide, which was critical for binding with calcium ions and promoting mineralization. The fifth element was a cell-targeting RGD motif. Self-assembly of this PA was used for effective mineralization. This amphiphile provided a reference for designing a PA for any desired application. The nanofibers are represented as cylindrical micelles, with alkyl tails on the inside and peptide segments on the outside in both β -sheet and α -helix configurations.

In contrast to traditional amphiphiles, supramolecular conjugates are constructed by combining two separate molecules through supramolecular interactions or dynamic covalent bonds. Supramolecular PA design commonly involves the host–guest chemistry of diverse macrocyclic hosts, including cyclodextrins, calixarenes, crown ethers, pillararenes, and cucurbiturils. Two-component and three-component supramolecular amphiphilic structures have been designed and constructed using this method. In 2009, Kros et al.⁴² reported a two-component vesicle formed by lipid-functionalized β -cyclodextrin and an N-terminal adamantane-functionalized octapeptide (VE)₄. The vesicle was transformed into a fiber-like structure at pH 5, which had the potential for controlled release. Cucurbit[8]uril (CB[8]) can accommodate two different guests inside its hydrophobic cavity, rendering it suitable for designing a three-component amphiphilic structure. Scherman et al.⁴³ constructed a supramolecular PA, which self-assembled to vesicles, using the ternary complexation of CB[8] (Figure 3B). Inside the CB[8] cavity, a pyrene-modified short hydrophilic peptide and a viologen-labeled lipid were inserted simultaneously, which responded to various external triggers. The tripartite also achieved fluorescence “switching on/off”.

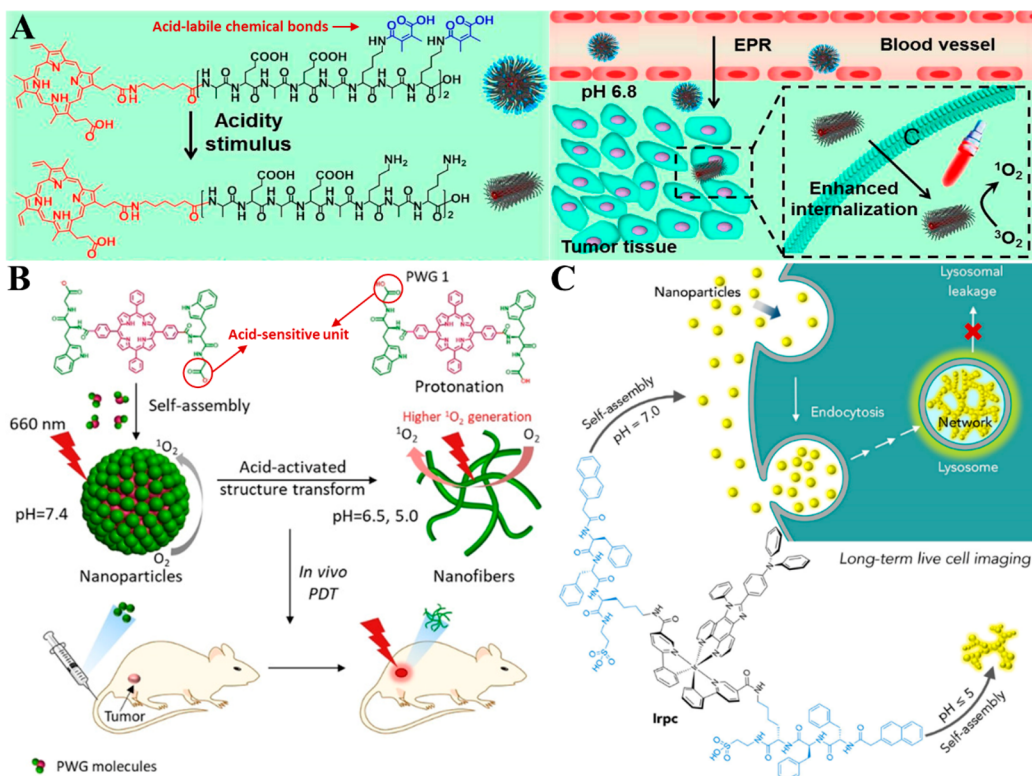


Figure 4. Schematic illustration of pH-responsive SAP nanoparticles. SAP nanoparticles achieve morphological transformation in special environments like tumor microenvironment (TME) or lysosome through acid-labile chemical bonds or acid sensitive units. (A) Nanoparticles transformed into nanofibers in TME through acid-labile chemical bonds. Adapted with permission from ref 58. Copyright 2017 American Chemical Society. (B) Carboxyl group of glycine as acid-sensitive unit to realize the transformation process. Adapted with permission from ref 60. Copyright 2020 The Authors, published by Wiley-VCH GmbH. (C) Morphological transformation occurred in lysosomes and long-term retention was realized. Adapted with permission from ref 61. Copyright 2021 Wiley-VCH GmbH.

Based on these mechanisms of self-assembled behavior, the morphological transformation of SAP can be explained. β -Sheets are known to assemble into fibrous structures. This trend can be broken by introducing the α -helices, amphiphiles, or the extra repulsion to disrupt the equilibrium between β -sheets, resulting in the formation of nanoparticles or micelles. Once the additional force is removed, a morphological transition occurs. As for amphiphiles, the separation of hydrophilic and hydrophobic parts can lead to disassembly. The solubility of some peptides is susceptible to temperature changes, leading to conversion between hydrophilicity and hydrophobicity, causing morphological changes. Basically, the morphological transformation of SAP is a macroscopic manifestation of remodeling the balance of inter/intra-molecular forces.

STIMULI-RESPONSIVE SAP NANOPARTICLES

Internal and external stimuli cause variations in the self-assembly feature or chemical composition of SAP nanoparticles.⁴⁴ Diseased tissue is distinct from healthy tissue with differentiated pH and protein expression profiles, therefore providing internal or endogenous stimuli, such as pH, temperature, and enzymes,^{45,46} whereas light,⁴⁷ magnetism,⁴⁸ or electricity⁴⁹ are external stimuli. Under stimuli operation, smart peptides can self-assemble, disassemble, or change their morphology depending on the chemical bond,⁵⁰ protonation degree,⁵¹ or solubility.⁵² The responsiveness of SAP nanoparticles to stimuli lays the foundation for biomedical applications. The required responsive model is different for

different applications. SAPs that aggregate *in situ* upon stimulation are beneficial for the aggregation-induced emission of disease diagnostic dyes or self-assembly mediated cytotoxicity for tumor therapy.⁵³ *In situ* assembly allows to tailor the materials to meet the functional requirements under the various physiological conditions, e.g., during circulation vs at the target site. In contrast, drug release depends on the disassembly process of SAP nanocarriers.^{54,55}

pH-Responsive SAP Nanoparticles. The formation of highly ordered SAP nanoparticles results from the cooperation among multiple noncovalent forces, including hydrogen bonds, hydrophobic and hydrophilic interactions, electrostatic interactions, and van der Waals force.⁵⁶ The disruption of the balance between the driving forces can change the self-assembly mode and morphology of SAP nanoparticles. pH affects the balance by regulating protonation/deprotonation or cleaving labile chemical bonds. For example, by incorporating Glu or Orn into the primary structure of Q11 peptide, the isotropic fluid-to-nematic transitions can be triggered by relatively small additions of acids or bases.⁵⁷

Tumor microenvironment (TME) and lysosomes have an acidic pH,^{58,59} rendering them suitable for designing acid-labile SAP nanoparticles for targeted imaging or therapy (Figure 4A). Jan et al.⁶⁰ presented an acid-activatable peptide-based nanosystem for photodynamic therapy (PDT), which comprised a dipeptide (tryptophan-glycine, WG) and a porphyrin (photosensitizers) (Figure 4B). Tryptophan provided delocalized π electrons for fluorescence, and the glycine-containing carboxyl group functioned as an acid-sensitive unit.

Table 1. Summary of Studies on Enzyme-Instructed Self-Assembly

Enzyme	Substrate	Tissue specificity	Application	Ref
MMP	FFALGLAGKK	—	<i>In situ</i> imaging	63
ALP	NBD-GFF-pY-ss-ERGD ^a	Tumor cells	Cancer diagnostics and therapy	64
ENTK	DYKDDDDK	Tumor cells	Cancer therapy	66
Cathepsin B	GFLG	Tumor cells	Cancer therapy	67
Gelatinase	PLGVRG	Gelatinase-positive bacteria	Recurrence tissue engineering/biosensing/bioimaging/gene or drug delivery	68
Caspase-3/7	DEVD	Tumor cells	Drug delivery/image-guided surgery	69
MMP-2/9	PLGYLG	Tumor cells	Image-guided surgery	76
ALP	Nap ^D F ^D pYX ^a	Tumor cells	Cancer therapy	73
ALP	NBD-ff-s-phosphate	Tumor cells	Cancer therapy	72
CES	NapFF-ester bond-taurine	Tumor cells	Cancer therapy	70
ENTK	DDDDK	Mitochondria of cancer cells	Mitochondria-specific drug delivery	71
Cathepsin B	GFLG	Tumor cells	Cancer therapy	78
Cathepsin B	GFLG	Tumor cells	Multidrug resistance	80
MMP	GPLGVRG	Tumor cells	Inflammatory disorders/tumors after surgery	81
SIRT5	Succinylated lysine	Mitochondrion	Live cell imaging/cancer therapy	82
ALP	KpY	Tumor cells	Cancer therapy	83
Tyrosinase	Y	Melanoma	Cancer therapy	84
Human kallikrein 2	GKAFRR	Tumor cells	Cancer therapy	85

^apY indicates phosphorylated tyrosine.

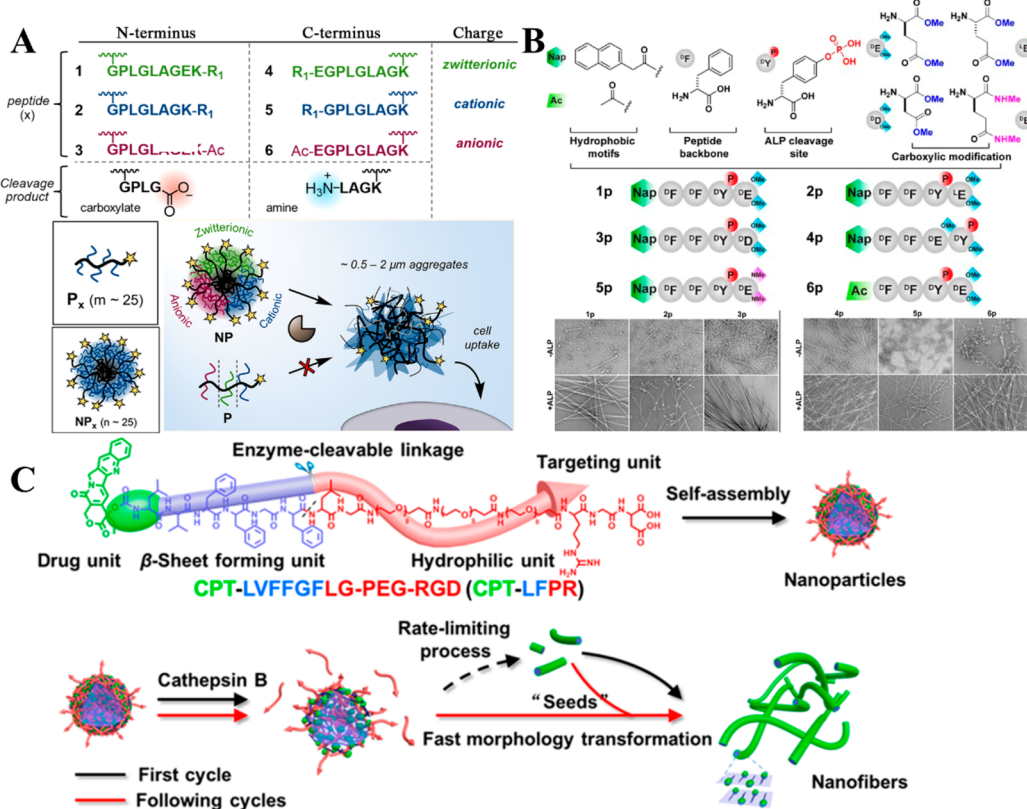


Figure 5. Schematic illustration of enzyme-responsive SAP nanoparticles. (A) MMP-9 enzymatic reaction led to morphological transformation of SAPs and promoted macrophage uptake. Adapted with permission from ref 74. Copyright 2017 American Chemical Society. (B) ALP catalyzed self-assembly of precursor molecular analogs into different forms. Adapted with permission from ref 73. Copyright 2017 American Chemical Society. (C) Cathepsin B catalyzed the peeling off of the PEG shell to promote the formation of fibrils, which acted as the seeds of fiber aggregation, so as to build a fiber drug library *in situ*. Adapted with permission from ref 78. Copyright 2019 American Chemical Society.

All-atom molecular dynamic (AAMD) simulations combined with the equivalence point and pK_a value showed that weak intramolecular hydrogen and high repulsion between the deprotonated peptide-porphyrin conjugates (PWGs) favored

nanoparticle formation under physiological conditions (pH 7.4). The protonated carboxyl groups of PWG resulted in a stronger intermolecular hydrogen bond in the acidic tumor microenvironment (pH 6.5), transforming the nanoparticles

into nanofibers. This peptide-porphyrin platform achieved an excellent tumor-imaging effect and a high PDT efficacy.

Long-term tracking is an emerging hot spot of bioimaging. To create a super stable lysosomal probe for long-term live cell imaging, Zhang et al.⁶¹ developed an aromatic-peptide-conjugated cyclometalated iridium(III) complex called Irpc (Figure 4C). The phosphorescent cyclometalated iridium(III) complex possessed aggregation-induced emission (AIE), which enabled stable fluorescence. Two aromatic-peptide-based building blocks (naphthalene-Phe-Phe-Lys, NapFFK) were used to promote self-assembly. Upon acid stimulation, Irpc transformed from scattered large nanoparticles (at pH 8 or 7) to smaller particles (pH 6) and formed interlinked networks (pH 5 or 4). In contrast to the prevailing pH-responsive SAP nanoparticles, the transition process was irreversible, endowing Irpc with much higher stability. Collectively, Irpc achieved long-term lysosome tracking even after more than 15 cell generations.

Conventional protonation or deprotonation tuned by the pH directly affects the SAP aggregation tendency. Chen et al.⁶² provided an alternative protocol for developing pH-sensitive SAP nanoparticles in which an acid-responsive shielding layer was introduced. This shielding layer prevented nanoparticles from aggregating into nanofibers by covering the doxorubicin (Dox)-peptide conjugate nanoparticles (DPC-NPs) through electrostatic interactions to avoid π - π stacking interactions and hydrogen bonding between the DPC-NPs. Therefore, the DPC-NPs were spherical and stable during blood circulation. After arriving at TME, DPC-NPs removed the shielding layer triggered by the slightly acidic condition, thus self-assembling itself into nanofibers and accumulating in the tumor tissue. The TME-responsive transformation of morphology enhanced the drug retention efficacy and exhibited a more specific tumor therapeutic outcome.

Enzyme-Responsive SAP Nanoparticles. Enzymes serve as endogenous stimuli, working directly on the chemical bonds between peptides or bridging molecules between compounds and peptides. Enzymes of relevance include matrix metalloproteinases (MMPs),⁶³ alkaline phosphatases (ALPs),⁶⁴ carboxylesterases (CESs),⁶⁵ enterokinases (ENTKs),⁶⁶ cathepsin B,⁶⁷ gelatinases,⁶⁸ and caspases.⁶⁹ The selection of disease-specific enzymes endows enzyme-responsive SAP with diagnostic or therapeutic abilities (Table 1). Enzyme-triggered self-assembly can serve as a signal amplification method to improve the signal-to-noise ratio or cytotoxic fiber-forming strategies for tumor-specific killing. It is worth noting that Xu et al. conducted pioneering studies in EISA.⁵⁰ They developed EISA nanoparticles using enzymes like CES,^{65,70} ENTK^{66,71} and ALP.^{72,73} Some of their excellent works are listed in detail below.

MMPs are extensively involved in perpetual extracellular matrix remodeling within diseased tissues and are identified as key molecular targets of myocardial infarction, hind limb ischemia, and cancer of all types.⁷⁴ MMPs are hydrolases acting directly on peptide bonds; the sequence for MMP peptide substrate is PX₁GLX₂G, where X₁ or X₂ represents a single amino acid with no significant preferences. MMPs specifically cleave amino bonds between G and L (Figure 5A).⁷⁵ Xu et al.⁷⁶ synthesized an *in situ* self-assembled near-infrared (NIR) peptide probe (TER-SA) with a tumor-specific excretion-retarded (TER) effect. TER-SA was cleaved by MMP-2/9 and then transformed into nanofibers with an antiparallel β -sheet conformation from a stable monomeric

state. The fiber-like structure allowed TER-SA to be retained for a long time in tumors, termed the TER effect. The peptide probe based on the TER strategy enabled high-performance imaging of human renal cell carcinoma and achieved complete tumor removal, ultimately reducing postoperative recurrence. MMP target sequencing can be integrated into nanoparticles as well as viral vectors to achieve tissue-specific gene delivery.⁷⁷

ALPs act as biomarkers in cancers such as osteosarcoma and cervical cancer.⁷³ ALPs conduct the cleaving of phosphate groups from phosphopeptides, thereby increasing hydrophobicity. Typically, phosphorylated Phe- and Tyr-containing tetrapeptide with an N-terminus modified with an aromatic group function as an ALP substrate (Figure 5B). Xu et al.⁷² developed a platform based on ALP-catalyzed assemblies that instantly targeted the Golgi apparatus (GA) and selectively killed cancer cells. An oxygen atom in the phosphodiester bond in a phosphopeptide (pO1) was replaced with a sulfur atom to generate a thiophosphopeptide (pS1). pS1 instantly accumulated in GA owing to the rapid ALP-catalyzed dephosphorylation and disulfide bond formation by itself and with Golgi proteins. pS1 transformed from micelles to nanofibers during dephosphorylation. In contrast, pO1 took a long time for dephosphorylation and cellular uptake and largely remained in the endosomes. The pS1 selectively inhibited HeLa cells ($IC_{50} = 2.8 \mu M$) and targeted Golgi for specific imaging.

CESs specifically cleave carboxylate bonds conjugated to peptides via chemical synthesis. Xu et al.⁷⁰ developed a pair of enantiomeric dipeptides conjugated with taurine via carboxylate bonds to examine the relationship between CES activities and the cancer inhibition efficacy of conjugates. After hydrolysis by CES, the corresponding products, dipeptides, self-assembled into nanofibers. The nanofibers selectively inhibited cancer cells exhibiting relatively high CES activity, and the inhibition efficacy was correlated with CES activities. Although CES was present in normal cells, the dipeptides were largely innocuous in normal cells because of the lower rate of EISA compared to tumor cells.

ENTK, an enteropeptidase, specifically cleaves peptides with a DDDDK sequence. Xu et al.⁷¹ reported enzymatic self-assembled branched peptides for targeting mitochondria and delivering cargo to mitochondria. The branched peptides transformed from micelles to nanofibers upon cleavage by intracellular ENTK. The *in situ* nanofiber formation resulted in their localization in the mitochondria. In addition, the branched peptides boosted the cytotoxicity of Dox against Dox-resistant cancer cell lines because of the enhanced uptake of Dox and its interference with mitochondrial DNA.

Cathepsin B is overexpressed and secreted from the cells of malignant tumors and premalignant lesions while functioning as a lysosomal protease in normal cells and tissues.⁷⁹ The specific cleaving substrate of cathepsin B is a tetrapeptide comprising GFLG (Figure 5C).⁷⁸ Therefore, Zhang et al.⁸⁰ designed a transformable peptide (CTGP) that self-assembled on cell membranes for encapsulating cells and overcoming tumor multidrug resistance (MDR). After cleavage by cathepsin B, CTGP encapsulated with Dox (CTGP@DOX) transformed from nanomicelles to nanofibers. However, the release efficiency of Dox was <6% in 24 h upon cleavage, mainly because of the re-encapsulation of Dox by the formed nanofibers. This slow release of Dox contributed to 45-fold higher drug retention than that of free Dox. The CTGP@DOX nanofiber could anchor to the cell membrane via its 16-carbon alkyl chain to achieve cell encapsulation and restrict Dox efflux.

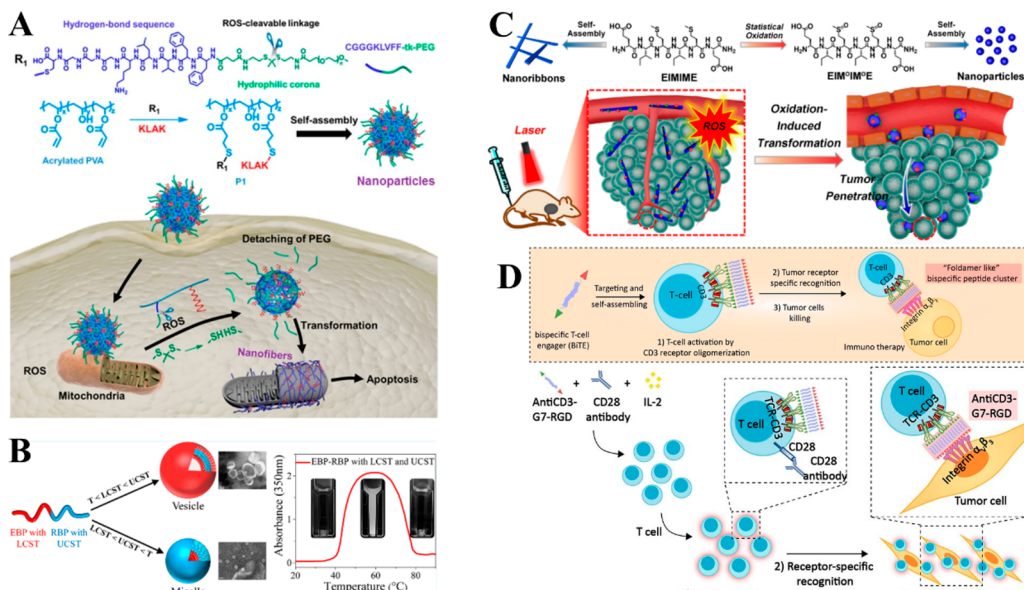


Figure 6. Schematic illustration of ROS/temperature/light/receptor-responsive SAP nanoparticles. (A) ROS-responsive fall away of PEG, leading to transformation of nanofibers and showing multivalent effect to enhance antitumor effect. Adapted with permission from ref 88. Copyright 2019 American Chemical Society. (B) Diblock copolypeptides composed of EBP with an LCST and RBP with a UCST showed converse phase transition behaviors with both a distinct LCST and a distinct UCST (LCST < UCST). Adapted with permission from ref 90. Copyright 2021 American Chemical Society. (C) ROS was produced after illumination to promote morphological transformation. Adapted with permission from ref 91. Copyright 2021 Elsevier Ltd. (D) Receptor-ligand responsive self-assemble led to peptide–protein complex oligomerization and concomitant T cell activation. Adapted with permission from ref 92. Copyright 2022 Wiley-VCH GmbH.

CTGP@DOX demonstrated 49-fold greater cytotoxicity to drug-resistant MCF-7R cells than free Dox.

Reactive Oxygen Species-Responsive SAP Nanoparticles. Overproduction of reactive oxygen species (ROS) is implicated in various chronic and degenerative diseases, including cancer⁸⁶ and also in neurodegenerative diseases.⁸⁷ In cancer cells, ROS is particularly overproduced in mitochondria. Wang et al.⁸⁸ made use of this feature and developed organelle-located morphology transformation polymer–peptide conjugates (PPCs) that could be triggered by endogenous ROS around the mitochondria to enhance multivalent cooperative interactions. PPCs included a poly(vinyl alcohol) backbone decorated with mitochondria-targeting cytotoxic peptide (KLAK) and β -sheet-forming peptide KLVFF tethered with hydrophilic PEG via a ROS-cleavable thioketal. Thioketal cleavage under overproduced ROS broke the hydrophilic/hydrophobic balance and induced PPC transformation from nanoparticles to nanofibers. As a result, the nanofibers with exposure of KLAK exhibited enhanced multivalent cooperative interactions with mitochondria, causing selective cytotoxicity against cancer cells and powerful tumor suppression efficacy *in vivo* (Figure 6A). Dong et al.⁸⁹ combined the GSH-responsive supramolecular assemblies with multivalent ligand presentation to enhance cancer cell targeting specificity and sensitivity. The main component was the targeting ligand-conjugated self-assembling monomer precursor (SAM-P), which existed as a monomer to provide strong electrostatic repulsion between cationic domains. The cleavage of the cationic domain mediated by GSH initiated self-assembly to form multivalent ligands for enhanced tumor recognition. This strategy could be potentially used in cell-specific molecular imaging and as a therapeutic agent with high sensitivity and specificity.

Temperature-Responsive SAP Nanoparticles. The hyperthermal environment in inflamed pathological sites or

external temperature operation is widely applied as a stimulus for manipulating the thermos-responsiveness of SAP nanoparticles. Like traditional thermoresponsive polymers, several peptides possess typical phase separation at temperature lower than the upper critical solution temperature (UCST) or higher than the lower critical solution temperature (LCST). The thermoresponsive SAP nanoparticles with LCST behavior will accumulate and achieve a sustained drug release at the target sites at a relatively high temperature;⁹³ however, those with UCST behavior produce a rapid release under the same conditions.⁹⁴ Moreover, the di- or multiblock copolymers combining LCST with UCST peptides exhibit a versatile thermoresponsive model. Copolymers whose UCST is lower than LCST undergo insoluble–soluble–insoluble transitions with increasing temperature. In contrast, polymers whose UCST is higher than LCST undergo soluble–insoluble–soluble transitions.⁹⁵ The most classical thermoresponsive peptides are elastin-based polypeptides (EBPs) that are composed of the repeated pentapeptide sequence I/V-P-G/A-X-G, where X is any amino acid apart from proline.⁹⁶ ELPs show LCST behavior and are widely used in tissue engineering, drug delivery, and protein expression and purification. Lim et al.⁹⁰ conjugated ELPs with resilin-based polypeptides (RBPs) with UCST behavior. Hydrophobic EBPs were selected to ensure that the LCST was lower than UCST of the EBP-RBP diblocks. When temperature was below UCST and LCST, the diblocks self-assembled into vesicles or micelles, which were determined by the number of pentapeptide repeats in the EBPs. However, they showed an inverted micellar structure above the LCST and UCST while being aggregated between LCST and UCST (Figure 6B).

Light-Responsive SAP Nanoparticles. Light, an easily operated external stimulus, can be manipulated with spatiotemporal accuracy; through interventional radiology,

various organs and tissues are accessible. However, with the exception of fluorescent proteins, to date there are no identified peptides that afford photoresponsive abilities. The photolabile capacity of SAP nanoparticles usually depends on the conjugation of additional photoabsorbing compounds, such as photosensitizers or photothermal inducers. The photoresponsiveness of SAP nanoparticles essentially depends on ROS production or hyperthermal conditions. For example, Yu et al.⁹¹ reported the cascade therapy in which ROS was generated by a photodynamic process and subsequently activated a redox-responsive process. The transformable nanofiber was co-assembled using a methionine-containing hexapeptide (EIMIME) and its two derivatives functionalized with photosensitizers (chlorin e6, Ce6) or chemo drugs (camptothecin, CPT). Photoinduced *in situ* ROS generation by Ce6 led to methionine oxidation. The conversion from hydrophobic thioether to hydrophilic sulfoxide promoted the conformational transition from β -sheets to random coils and the morphological transition from nanofibers to nanoparticles. This transition improved the cellular internalization and tumor penetration of the scaffolds. The CPT moiety, which was covalently connected to the peptide via a GSH-responsive disulfide linkage, was released in the presence of GSH in cancer cells. The cascade therapy also achieved efficient tumor inhibition *in vivo* (Figure 6C). In addition to exerting PDT alone, SAP nanoparticles are generally tailored to other stimuli-responsive processes. Yu et al.²¹ designed a chimeric peptide, CMP-PpIX, by combining a photosensitizer-peptide conjugate and a caspase-3-sensitive sequence to achieve enhanced PDT and *in situ* therapeutic feedback. The conjugate C₁₆-K(PpIX)-GRRRR-AEEA-K(FAM)SDEVDSK(Dabcyll)PEG₈PEG₈ comprised protoporphyrin (PpIX) as the photosensitizer, palmitic acid as the membrane insert motif, R₄ as a cell-adherent peptide, DEVD as a caspase-3/7 responsive peptide, Dabcyll and FAM as a Förster resonance energy transfer (FRET) fluorophore pair, and PEG₈-PEG₈ as a hydrophilic shell. ROS produced by CMP-PpIX under irradiation directly damaged the cell membrane and rapidly induced apoptosis after being attached to the cell membrane using R₄ peptide and lipophilic palmitic acid. The apoptosis-induced activation of caspase-3 cleaved CMP-PpIX to separate FAM and Dabcyll. Before cleavage by caspase-3, FAM fluorescence was quenched by Dabcyll. Therefore, increased fluorescence intensity indicated the production of activated caspase-3 to feedback real-time PDT therapeutic efficacy. Recently, Zou et al.⁹⁷ developed a light-triggered platform. This platform comprised a targeting peptide (RGD), a supplied H-bonding peptide (KLVFF), and light-responsive unit (3-methylene-2-(quinolin-8-yl) isoindolin-1-one (MQIO) derivatives. The transformation from nanoparticles to nanofibers through H-bonding interactions of KLVFF peptide was caused by the molecule sliding occurred after conformation changes of MQIO unit.

Other Stimuli-Responsive SAP Nanoparticles. Other stimuli, such as metal ions,^{98,99} solvents,^{100,101} small compounds,^{102,103} and ligand–receptor interactions,^{92,104} provide excellent functional transformation of SAP nanoparticles. Metal elements (e.g., calcium, zinc, iron, and copper), which are indispensable components of life, exist widely *in vivo*. Tao et al.¹⁰⁵ constructed a three-stage self-assembled nanoband-aid (NBA) that responded to calcium ions and blood coagulation factors. NBA comprised two functionalized peptides: Ca²⁺ binding peptide (CBP) and cross-linking peptide (CRP). CBP comprised (RADA)₄ linked to a Ca²⁺-binding sequence

(GSQLGYIQIR). CRP was composed of (RADA)₄ fused with a cross-linking motif (GGQQLK). CBP and CRP co-assembled into nanofibers and formed a mesh-like network after coordination with calcium ions under aqueous conditions. When catalyzed by the blood coagulation factor, NBA further underwent the third stage, self-assembling into a densely compacted physical barrier to stop and control bleeding. As a result, NBA rapidly and efficiently stopped bleeding from rat liver scratches.

Some metal ions are rich in specific tissues; zinc ions are abundant in prostate tissue, which is approximately 10-fold higher than that in other soft tissues.¹⁹ Zhong et al.¹⁰⁶ developed a series of self-assembled forkly peptides (E₃F_n) utilizing this feature. The three adjacent glutamic residues, forming a forkly fragment, could chelate zinc ions and promote the formation of supramolecular hydrogels. Since other cationic ions failed to trigger hydrogel formation at physiological concentrations, the forkly peptides were injectable and achieved a prostate tissue-specific self-assembly *in situ*. The E₃F₃ hydrogels exhibited optimal gelation time, satisfactory mechanical strength, and excellent thixotropic properties among all groups.

Ligand–receptor interactions exist widely in biological systems. Some diseases overexpress certain receptors, such as folate receptors overexpressed in ovarian cancer cells. Highly specific SAPs can be developed using ligand–receptor interactions. Wang et al.⁹² developed a bispecific assembling peptide (antiCD3-G7-RGD). Upon binding to the cell membrane receptor, peptide conformation was stabilized along with decreased self-assembly activation energy, promoting CD3 oligomerization and T cell activation, leading to T cell-mediated cancer cell cytosis (Figure 6D). Lam et al.¹⁰⁴ developed transformable peptide nanoparticles by integrating the HER2-binding domain (YCDGFYACYMDV), which could interact with the HER2 receptor overexpressed in breast cancers. Upon interaction with HER2 displayed on the tumor cell surface, the nanoparticles could transform into a fibrillar structural network *in situ*, suppressing HER2 dimerization and killing tumor cells. This receptor-mediated transformable peptide nanoplateform has great clinical potential.

SMART SAPS FOR THERAPY

The bottom-up synthesis of SAP nanoparticles provides an interesting and attractive approach for developing other nanobiomaterials.¹⁰⁷ SAPs, especially molecularly stimuli-responsive SAPs, with properties such as biocompatibility, biodegradability, flexible responsiveness, and specific biological function, are extensively developed for biomedicine and tissue repair. There are about 80 peptide drugs on the global market, especially for treatment of cancer (18%), metabolic disorders (17%), and other medical conditions.¹⁷ There are more than 150 peptides that are in the clinical development stage, and another 400–600 peptides that are in the preclinical research stage.¹⁰⁸ More than 2000 clinical trials were carried out based on therapeutic peptides.¹⁷ Peptide drugs are gradually attracting the attention of pharmaceutical companies. However, development of these peptide drugs is also troubled by some problems like *in vivo* stability, targeting ability, and so on. Developing stimuli-responsive SAPs is one of the most powerful ways to solve the current problems.

Smart SAPs for Anticancer Therapy. Cancer is characterized by the unrestricted proliferation of transformed cells. Tumor cells compete for nutrients and oxygen in the

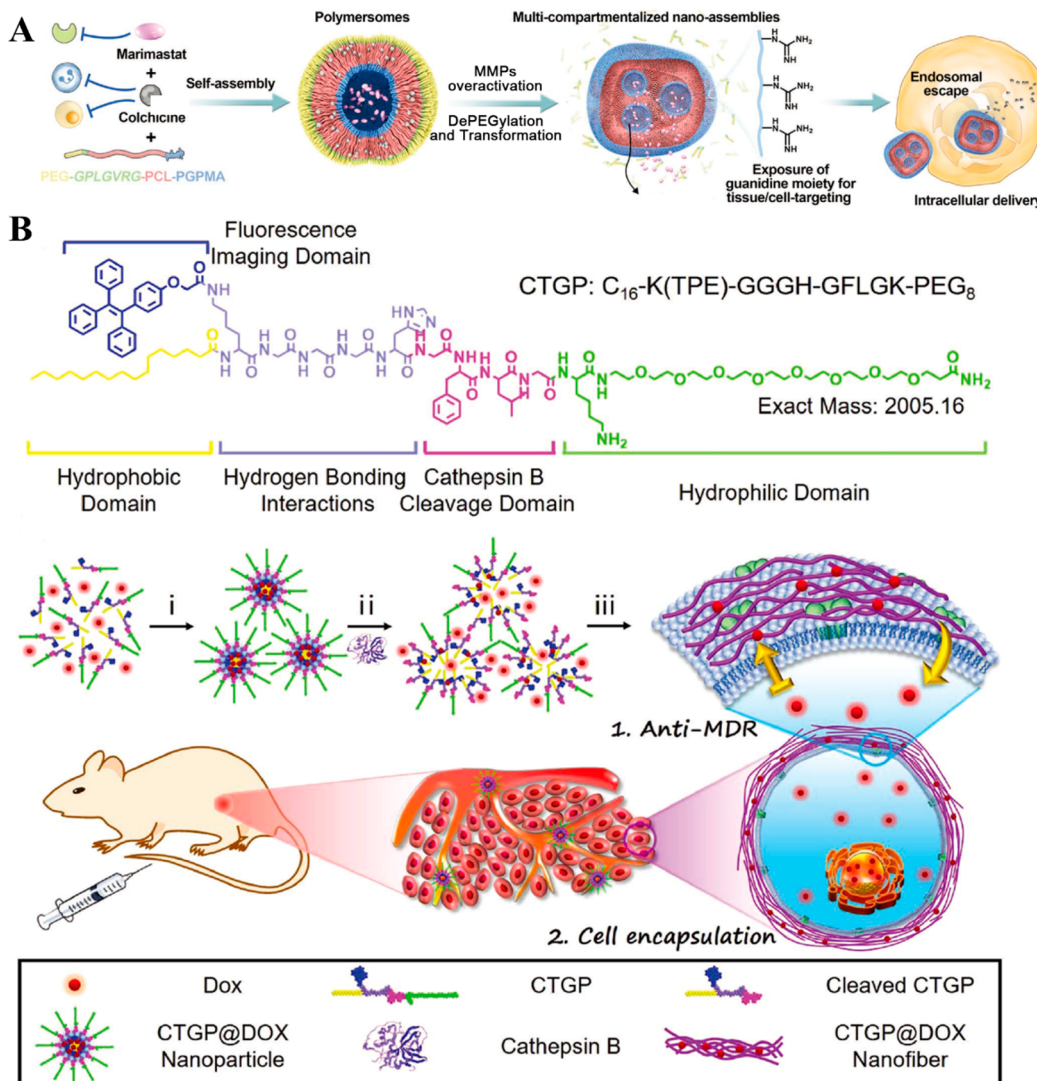


Figure 7. Schematic illustration of SAPs mediated antitumor effects. (A) SAPs as delivery vectors for colchicine and marimastat in the treatment of metastatic breast cancer. Adapted with permission from ref 81. Copyright 2021 Wiley-VCH GmbH. (B) Responsive self-assembly of SAPs into nanofibers to effectively encapsulate cells, improve antitumor effects, and counter multidrug resistance. Adapted with permission from ref 80. Copyright 2018 Wiley-VCH Verlag GmbH & Co. KGaA, Weinheim.

blood. Hypoxia, lower pH values, the overexpression of some enzymes, and the increased secretion of specific cytokines can be observed in TME. These factors trigger endothelial cell proliferation, lead to angiogenesis, and allow tumor cells to enter the circulatory system, causing tumor metastasis. Within the TME, tumor-induced immunosuppression allows aggressive tumors to evade the immune system.^{109,110} This pathophysiology however also presents an opportunity to design smart SAPs that can respond and adapt to the microenvironment-specific stimuli to perform desired functions. SAPs can serve as targeted delivery vehicles for a multitude of medically relevant cargo, such as chemotherapy (cyclophosphamide, methotrexate, doxorubicin, etoposide, and paclitaxel), nucleic acids (siRNA, miRNA, mRNA, and DNA), and photosensitizers (PDT and PTT: protoporphyrin, Ce6).¹¹¹ Some peptides included in SAPs also serve as the therapeutic agents. For example, SAPs have been designed to assemble as nanofibers twined around the cells/organelle to prevent tumor metastasis or cause cell death.⁸⁸ For tumor-induced immunosuppression, SAPs have also been developed

to target tumor cells or antigen-presenting cells (APCs) to activate local or systemic immune responses.^{112,113}

SAPs utilize a bottom-up strategy to create exquisite nanosized delivery systems¹¹⁴ that enable them to carry cargo with high loading and low leakage. The stimuli-responsive properties of SAPs enable tumor-targeted and programmable cargo release.¹¹⁵ SAPs help deliver chemotherapeutic drugs, such as doxorubicin,¹¹⁶ sorafenib,¹¹⁷ colchicine,⁸¹ and paclitaxel,¹¹⁸ thereby improving solubility, reducing systemic toxicity, prolonging the retention time at tumor sites, and increasing antitumor activity (Figure 7A). Wu et al.¹¹⁹ developed a multifunctional peptide (P51) for programmed pirarubicin delivery. P51 was responsive to an acidic environment, a reducing agent, and MMP-2 via disrupting the interaction between peptides and pirarubicin, a disulfide linkage, and the peptide PVGLIG. *In vitro* and *in vivo* results showed more effective tumor targeting, antitumor effects, and reduced systemic toxicity of P51 NPs. Gene therapy is a promising method to treat tumors. Delivering negatively charged DNA/RNA to tumor cells through SAPs

Table 2. Representative Therapeutic Peptides Employed for Cancer Treatment

Name	Sequence	Function site	Antitumor mechanism	Ref
KLA	(KLAKLAK) ₂	Mitochondrion	Induce mitochondrial dysfunction	125, 126, 128
Melittin	GIGAVLKVLTTGLPALISWIKRKRQQ-NH ₂	Cell membrane	Increase the permeability of cell membrane and release the contents	127, 129
C16Y	DFKLFAVYIKYR	Cell membrane	Target integrin $\alpha_5\beta_3$ and $\alpha_5\beta_1$ to inhibit angiogenesis and tumor growth	130
G0-203	R9-cqcrkn	Intracellular	Block intracellular MUC1 function, compromise the redox balance in cells	131

requires positively charged amino acids. SAPs protect nucleic acids against digestion by plasma and serum nucleases. Nanocarriers with a positive surface charge can be easily cleared from the circulation through the reticular endothelial system (RES); therefore, a shielding layer, such as hyaluronic acid (HA),¹²⁰ and other methods have been employed to convert surface charge. Li et al.¹²¹ designed an amphipathic peptide chimera to targeted delivery and release of siRNA, silencing the expression of tumor-associated tissue factors. The highly cationic repeating arginine-arginine-serine (RRS) segment of this amphipathic peptide was included to absorb RNA molecules electrostatically. The surface charge significantly decreased from 13.3 mV to -9.9 mV after incorporating the siRNA and favored an increased circulation half-life. The polyhistidine moiety, which was responsive to the acidic TME, induced surface charge reversion to facilitate cell uptake. siRNA decreased the invasive potential and platelet adhesion of cancer cells, preventing its distant metastasis and reversing the tumor-induced hypercoagulable state. Co-delivery of chemotherapeutic drugs and nucleic acids by SAPs helps treat tumors from multiple perspectives and exhibits synergistic effects. Wang et al.¹²² developed a self-assembled nanoprodrug platform with synergistic effects of cisplatin and RNAi to fight cisplatin-resistant lung cancer. This platform fastened Pt(IV) via amide bonds and allowed the rapid release of active platinum ions (Pt(II)) in the presence of GSH. Beclin1 siRNA was delivered into the cytoplasm through this cationic carrier and inhibited autophagy. This platform was developed to fight against cisplatin-resistant lung cancer and possessed favorable antitumor effects. Photosensitizer is key to the PDT and PTT. The retention time of photosensitizer will be extended when smart SAPs enter the TME and are converted from nanoparticles to nanofibers. This long-term retention leads to massive accumulation at tumor sites, exhibiting an excellent antitumor efficacy.⁵⁸ He et al.¹²³ synthesized a chimeric peptide called TRFC to deliver Ce6. Upon light irradiation, the ROS produced by Ce6 induced oligoarginine oxidation to generate NO, driving the *in situ* nanosphere-to-nanorod transformations. The reaction between NO and ROS yielded peroxynitrite anions (ONOO⁻), which increased cytotoxicity, thereby amplifying the therapeutic outcome of PDT. Stimuli-responsive SAPs are conspicuous delivery systems that exert antitumor effects through chemotherapy, gene therapy, PDT, and PTT.

In addition to exerting the antitumor effect of SAPs via the delivered cargo, some peptides exert therapeutic effects. Some therapeutic peptides were discovered in nature, whereas others were screened in laboratories using peptide library.¹²⁴ Representative therapeutic peptides employed for cancer treatment are listed in Table 2. The proapoptotic peptide [KLAKLAK]₂ (KLA), a common therapeutic peptide, selectively targets and destroys mitochondrial membranes and induces mitochondrial dysfunction. Recently, some SAPs

integrated KLA to treat tumors by simultaneously playing the role of building blocks, therapeutic peptides, and cell-penetrating peptides.^{125,126} Melittin, a cationic host defense peptide, can induce tumor apoptosis by disrupting cell membranes, followed by releasing intracellular contents, such as whole-tumor antigens and damage-associated molecular patterns, exhibiting a certain immune regulation effect.¹¹² However, the strong hemolytic activity and nonselective cytotoxicity of melittin limit its use. Wu et al.¹²⁷ constructed dually responsive nanotransformers with nanosphere-nano-fiber-nanosphere transitions caused by the acidic TME as well as NIR laser irradiation. The net-like nanofibers contributed to long-term retention in tumor tissue and inhibition of tumor cell metastasis to distant organs. With the help of external NIR laser irradiation, PTT was activated, followed by the transformation between nanofibers and nanospheres, which ensured the deep penetration of MEL peptide for effective tumor eradication.

Another strategy of therapeutic SAPs is to make use of dynamic self-assembly from monomers into nanofibers at the target site to induce desired effects on the cells or organelles. To achieve these properties, it is essential to incorporate motifs that stimulate nanofiber formation, such as β -sheet motifs, into SAPs. Typical short peptides with this ability include EAK16, RADA16, KLD-12,¹³² KLVFF,¹³³ and KGFRWR.¹³⁴ SAPs transform into nanofibers around organelles through rational design, destroy organelles, and induce cancer cell death. Lam et al.¹³⁵ reported the peptide (CPTNP) containing all D-amino acids (kffvlk) transformed into nanofibers in lysosome due to the shift in $\pi-\pi$ interaction between phenylalanine side chains, and therefore inducing lysosomal membrane permeabilization. Based on these properties, CPTNPs could treat tumors and sensitize tumor cells to cisplatin activity. The process of transforming SAPs into nanofibers can also take place extracellularly, thus preventing tumor angiogenesis and metastasis.¹³⁶ Nanofiber transformation combined with chemotherapy shows sustained release properties, inhibits tumor growth *in situ*, and effectively prevents metastasis.¹³⁴ Transformable chimeric peptides for cell encapsulation can also overcome multidrug resistance (MDR). Zhang et al.⁸⁰ reported that chimeric peptide (CTGP) transformed into nanofibers using cathepsin B restricted the loaded DOX efflux. This behavior counteracted P-glycoprotein-mediated drug efflux and overcame MDR (Figure 7B). In addition, SAPs can also respond to ligand-receptor interactions to form nanofibers, which block signaling pathways and exhibit excellent antitumor effects.⁹² The transformed nanofibers can also be used to efficiently interrupt the PD-1/PD-L1 interaction in immune checkpoint therapy, breaking the limitation of poor blocking efficiency.¹³⁷

Smart SAPs for Antibacterial Therapy. Bacterial infections, especially those caused by drug-resistant bacteria, have attracted the attention of researchers. SAPs can achieve

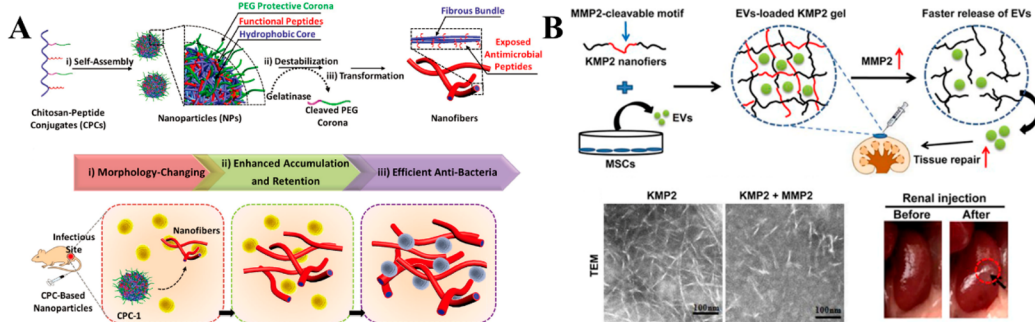


Figure 8. Schematic illustration of approaches that show the antibacterial/tissue repair effects of SAPs. (A) Efficient antibacterial effects of SAPs responsive to gelatinase. Adapted with permission from ref 146. Copyright 2017 Wiley-VCH Verlag GmbH & Co. KGaA, Weinheim. (B) MMP responsive SAP hydrogel as an enhanced cell-free therapy for tissue regeneration. Adapted with permission from ref 149. Copyright 2019 Elsevier B.V.

deep penetration, controlled release, and specific targeting of antibiotics when used as delivery systems, thereby reducing the administered dose, improving drug efficacy, and weakening drug resistance. Chmielewski et al.¹³⁸ reported a cleavable conjugate with efficient mammalian cell penetration and intracellular pathogenic bacteria clearance ability. This conjugate was composed of kanamycin and a nonmembrane lytic antimicrobial peptide (P14LRR), which could form a cationic amphiphilic polyproline helix. Moreover, peptides, such as cationic host defense peptides (CHDP), also known as antimicrobial peptides (AMPs), have bactericidal effects by directly killing bacteria or affecting the dormitory against infection.^{139,140} SAPs have great potential for combating drug-resistant bacterial infections.¹⁴¹ Cationic AMPs interact with negatively charged bacterial membranes, increasing membrane permeability, disrupting cell membranes, and releasing cell contents. Other antibacterial mechanisms include inducing DNA damage, inhibiting protein synthesis and enzyme activity, and blocking cytoderm synthesis.¹⁴²

The development of molecularly stimuli-responsive SAPs that effectively target and kill bacteria without damaging mammalian cells is challenging. The bacterial infection site is usually locally acidic due to bacterial metabolism and host immune response.¹⁴³ Taking advantage of this feature, Chan-Park et al.¹⁴⁴ synthesized cationic and anionic peptidosaccharide copolymers that responded to low pH and self-assembled into nanomicelles to expose the antibacterial cationic peptide. Chitosan was used to achieve the targeting function of this nanomicelle. Antibiotics can also function as targeting agents. Vancomycin specifically binds to the D-Ala-D-Ala sequence in Gram-positive bacterial walls. As a result, various bacteria-specific diagnostic and therapeutic SAPs have been developed.^{145,147} Wang et al.¹⁴⁶ designed a chitosan-peptide conjugate (CPC), which contained a chitosan backbone, an enzyme-cleavable peptide with a PEG terminal, and an antibacterial peptide (KLAK) (Figure 8A). Under the function of gelatinase, CPC transformed from nanoparticles into nanofibers. The exposed α -helical structure of KLAK led to multivalent cooperative electrostatic interactions with bacteria and disruption of the cell membranes. This morphological transformation resulted in increased binding efficacy, effective accumulation, prolonged retention at the infection site, and enhanced antibacterial activity. Ligand–receptor interactions are an ideal option for targeted delivery. Wang et al.¹⁴⁷ designed a human defensin-6 (HD6) mimic peptide (HDMP), which self-assembled into entangled fibrous networks, trapped

microbial pathogens, and blocked invasion. The ligand peptide sequence RLYLRIGR impeded superior recognition functionality of HDMP compared to HD6 by binding to lipoteichoic acid (LTA), a component of Gram-positive bacteria. This transformation, triggered by ligand–receptor interactions, precisely mimicked the antibacterial process of HD6 and safely and effectively inhibited Gram-positive bacterial infection *in vivo*. Combination therapies using SAPs were also developed. Biomimetic SAPs loaded with antibacterial Ce³⁺ rapidly co-assembled into a hydrogel network structure *in situ* driven by Ca²⁺. This hydrogel reduced inflammatory responses by blocking bacterial infection and promoted wound healing and thus facilitating hemostatic and antibacterial properties.¹⁴⁸

Smart SAPs for Tissue Repair. Tissue repair mainly involves hemostasis, infection and inflammation, angiogenesis, and re-epithelialization.¹⁵⁰ Several factors can be used as stimuli for molecularly stimuli-responsive SAPs, such as transglutaminase factor XIIIa during blood clotting, the higher temperature at the inflammation site, and MMPs involved in ischemic injury and tissue repair. For tissue repair, SAPs must be designed to self-assemble into hydrogels that can deliver payloads, mimic the extracellular matrix (ECM), and promote tissue repair. SAPs serve as delivery vectors for loading antimicrobials, vascular endothelial growth factor (VEGF), and neural bioactive ligands to maintain a healthy tissue-specific microenvironment and provide essential cytokines required for tissue repair.¹⁵¹

Hydrogels mimicking the ECM are promising materials for tissue repair. They provide a good environment for cell growth, allow multiple cell–cell and cell–matrix interactions, and promote cell proliferation, differentiation, migration and reprogramming.¹⁵² The common polypeptide sequences used to construct hydrogels for tissue repair include RGD, IKVAV, YIGSR, and RADA16.¹⁵³ IKVAV and YIGSR belong to the laminin-derived peptide motif family, which have major roles in cell attachment, migration, and adhesion.¹⁵⁴ The most significant peptide used to mimic the ECM is RGD, which is originally derived from fibronectin. RGD is the key regulator of cell–cell and cell–ECM communication. It boosts cell adhesion, migration, and differentiation and is strongly linked to tissue regeneration and embryonic development.¹⁵⁵ RADA16 hydrogels support the proliferation and differentiation of different types of cells.¹⁵⁶

The SAP hydrogels designed for tissue repair can be used in many aspects, such as bone, cartilage, and nerve regeneration.

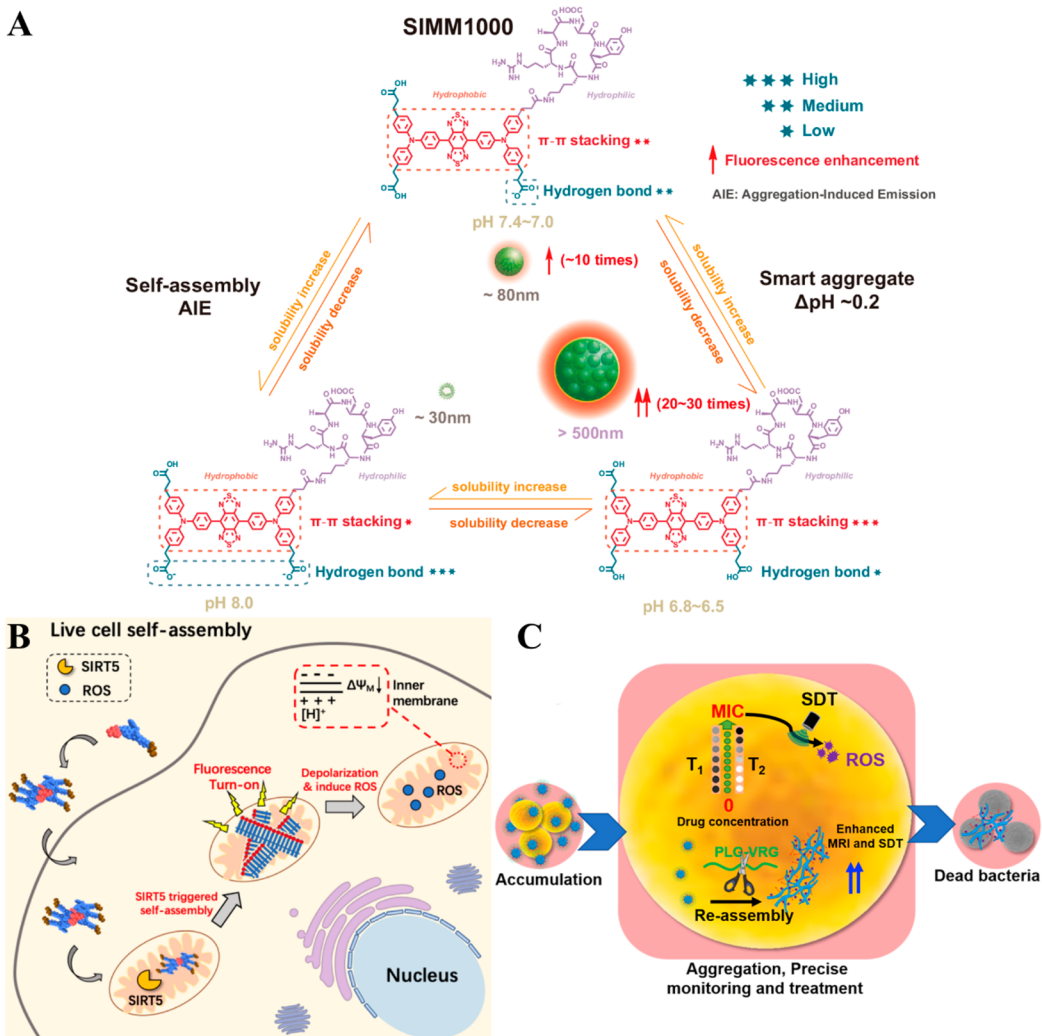


Figure 9. Schematic illustration of approaches to achieve targeted imaging for SAPs. (A) Self-aggregation of SIMM1000 in acidic TME *in situ* resulted in an extremely long tumor retention and a fluorescence enhancement. Adapted with permission from ref 164. Copyright 2021 Wiley-VCH GmbH. (B) The turning-on of SAP fluorescence upon forming nanofibers stimulated by SIRT5 (a mitochondria-localized enzyme). Adapted with permission from ref 82. Copyright 2020 American Chemical Society. (C) Enzyme-induced morphology transformation of nanoparticles for precise magnetic resonance imaging-guided treatment of drug-resistant bacterial deep infection. Adapted with permission from ref 170. Copyright 2021 Elsevier Ltd.

The response characteristics enable SAPs to be more accurately located at the site of tissue damage. Rodziewicz-Motowidlo et al.¹⁵⁷ linked peptide fibrils (QAGIVV) with active peptides that promote wound regeneration through neutrophil elastase sensitive sequences (AAPV) to form a peptide hybrid. This hybrid released active substances while constructing three-dimensional fiber scaffolds. The scaffolds promoted tissue repair and wound healing. QAGIVV can be replaced with other peptide fibrils, such as IKVAV. Visceral bleeding and penetrating wounds remain major challenges in emergency trauma treatment. Peptide nanofibers responsive to Ca^{2+} and blood coagulation factor XIIIa showed great potential in reducing inflammation and promoting wound healing after undergoing morphological transformation.¹⁰⁵ Combined with antimicrobials, hydrogels can prevent bacterial infections while promoting wound healing.¹⁴⁸ Unlike gel network formation, Liu et al.¹⁴⁹ developed a hydrogel delivery system for delivering mesenchymal stem cell-derived extracellular vesicles (MSC-EVs), which showed great potential for tissue repair. The MMP-2 sensitive SAP hydrogel extended the half-life of

MSC-EVs and exhibited controlled release properties at the desired sites. Compared to peptides or EVs alone, peptide-EVs showed better efficacy in promoting endothelial cell proliferation and angiogenesis. This study highlighted that EV-released peptide hydrogel was a promising cell-free therapy for tissue repair (Figure 8B).

Smart SAPs for Other Therapeutic Applications. SAPs have been widely used to treat many diseases owing to their excellent characteristics. Intrarenal SAP administration improves tissue repair after renal ischemia-reperfusion injury.¹⁵⁸ Intrahepatic SAP administration helps recover from hyperammonemia and damage in acute liver injury.¹⁵⁹ Intrapulmonary SAP administration enables *in vitro* and *in vivo* genome restoration of cystic fibrosis.¹⁶⁰ Molecularly stimulus-responsive SAPs realize morphological transformation at the lesion sites; hence, they are characterized by high safety, good targeting, and controlled release of payloads.

MMPs are overexpressed in ECM and are associated with many diseases, such as cancer and myocardial infarction (MI). Christman et al.¹⁶¹ designed MMP-responsive peptide-

polymer amphiphiles for MI, which underwent a morphological transition from discrete micellar nanoparticles into network-like scaffolds. Such amphiphiles realized targeted accumulation and prolonged retention in the heart tissue after MI and had potential to slow down or inhibit the progression of negative left ventricular remodeling. Smart SAPs improve the safety of organ-specific administration.

Tear fluid comprises functional components, such as soluble antibodies, mucous proteins, enzymes, and ions, and resembles serum in many aspects. Researchers have found that ALP expression in the tear fluid of patients with uveitis was much higher than those without uveitis. ALP-instructed self-assembly of SAPs in tear fluids offers a powerful strategy for the targeted and long-term accumulation of a therapeutic agent at the lesion site.^{162,163}

SMART SAPS FOR TARGETED IMAGING

Medical imaging technology plays an important role in the diagnosis and treatment of diseases. Imaging also plays a role in longitudinal follow up and stratifying whether patients respond to a therapy or not. Tumor treatment accuracy can be improved, diagnosis and treatment integration can be realized, and positive outcomes can be obtained through real-time monitoring of the tumor treatment process. The application of smart SAPs in imaging can enhance the sensitivity and accuracy of diagnosis through the following mechanism: (1) SAPs respond to tissue- or cell-specific biomarkers, thus enhancing the selectivity; (2) SAPs aggregate in the target site to exhibit different pharmacokinetics with free imaging agents, thus improving the signal-to-noise ratio; (3) SAPs can cooperate with aggregation-induced emission (AIE) dyes to further improve their sensitivity. Currently, smart SAPs are used in diverse diagnostic models, such as magnetic resonance imaging (MRI), optical imaging (OI), photoacoustic imaging (PAI), and multimodality imaging. Each imaging technology has its exclusive characteristics, which is described below.

Smart SAPs for Optical Imaging. Optical imaging includes two imaging modes: bioluminescence imaging and fluorescence imaging. As a noninvasive imaging technique, optical imaging can visually monitor the behavior of cells or genes in living organisms, in particular in preclinical development. It has the advantages of easy operation, intuitive results, high sensitivity, and a wide range of labeled objects. However, fluorescent agents do not usually exhibit selectivity for targets. The fusion of fluorescent agents with target motifs solves this problem. Smart imaging SAPs can improve the pharmacodynamic of the imaging agents and enable tissue-specific targeting and prevent washout effect and renal metabolism.¹⁷ Smart SAPs form nanoparticles in target sites, triggered by the indicated biomarkers, which enhance the signal-to-noise ratio by highly concentrated dyes (Figure 9A).¹⁶⁴

The selectivity of fluorescent agents combined with SAPs can be achieved by the responsiveness to internal environment, such as enzymes and pH, or genes and proteins in organisms. Sun et al.⁸² designed an amphipathic polypeptide precursor that responded to SIRT5, a mitochondria-localized enzyme. After entering the mitochondrial, Ksucc with a negative charge in the peptide was hydrolyzed by SIRT5 enzyme to form a zero-charge desuccinylated peptide, which promoted the self-assembly of polypeptide fragments rich in phenylalanine. Fluorophore NBD could generate strong fluorescence in a hydrophobic self-assembly environment and increase mitochondrial ROS, thus providing a useful idea of mitochondria-

confined peptide self-assembly for SIRT5 imaging and potential anticancer treatment (Figure 9B). Sun et al.⁶⁰ designed an acid-activatable peptide-based transmorphic nanosystem for PDT (Figure 4B). The protonation of peptide-porphyrin conjugate (PWG) owing to the increased acidity induced the transformation of nanoparticles into nanofibers. Strong fluorescent signals of these nanomaterials were detected in tumor tissue up to 7 days after administration. This *in situ* fibrillar transformation strategy achieved targeted long-term imaging and therapy.

NIR dyes, which have deep tissue penetration and low optical damage, emerged in living system imaging and are most used for *in situ* self-assembly. Owing to the photothermal characteristics of NIR dyes, they are often used in imaging-guided photothermal therapy. Wang et al.¹⁶⁵ used an all-hydrocarbon peptide stapling strategy to strengthen the α -helix structure of the peptide, which was coupled with an NIR-II fluorescent probe (N2) and self-assembled to realize tumor imaging. Furthermore, using two fluorescent reagents on SAPs can achieve different functions. Wang et al.¹⁶⁶ constructed probes of peptide-cyanine conjugates (P-1Cy and P-2Cy). The recognition motif of the peptide-cyanine conjugates specifically recognized the X-linked inhibitor of apoptosis protein (XIAP), leading to the activation of caspase-3/7. Then the enzymes caspase-3/7 cleaved enzymatically cleavable linker (DEVE), resulting in the *in situ* self-assembly of Pr-1Cy or Pr-2Cy (the self-assembled residue of P-1Cy or P-2Cy, respectively). The single cyanine (Pr-1Cy) or double cyanine (Pr-2Cy) substitution led to a different aggregation type, resulting in an energy conversion mode and making P-1Cy a NIR fluorescence imaging agent, while P-2Cy a photothermal therapeutic agent. NIR dye imaging can also be used for surgical treatment guided by accurate imaging such as the TER-SA probe developed by Xu et al.⁷⁶ This probe could *in situ* construct peptide-based nanofibers that exhibited an excretion-retarded effect in the kidney, enabling increased S/N ratio tumor imaging to guide high-performance tumor removal. The tumor-specific excretion-retarded (TER) effect also enabled the precise identification of eye-invisible tiny lesions (<1 mm), which contributed to complete tumor removal and significantly reduced the postoperative recurrence compared with traditional surgery, ultimately reducing the postoperative recurrence rate of renal cell carcinoma. Such an efficient fluorescent probe is suitable for tumor surgery in metabolic organs guided by accurate imaging.

In contrast to traditional fluorescent agents, which usually exhibit aggregation-causing quenching effects, AIE molecules emit enhanced and stable fluorescence upon aggregation. The combination of SAPs with AIE dyes enhances the sensitivity and stability of imaging. Li et al.¹⁶⁷ designed and synthesized a controllable *in situ* assembly nanostructure peptide-AIE conjugated probe, BIVE-TPE, for cell imaging. BIVE-TPE was consisted of a self-assembled peptide-tetraphenylethene (TPE) motif, a fibroblast activation protein alpha (FAP- α) responsive motif, a hydrophilic motif, and a targeting motif. The intramolecular movement of TPE could be strongly restricted by regulating the assembly of BIVE-TPE, so that the probe had a higher fluorescence signal output. The various nanostructures formed by peptide and TPE could enhance retention and accumulation on the surface of cells with better imaging window. AIE dyes can be used for not only tumor cell bioimaging but also guiding the accurate imaging of surgery. Chang et al.¹⁶⁸ proposed an efficient fluorescent probe MPA-

Ph-R-FFGYSA, in which YSA peptide specifically identified the overexpressed EphA2 receptor in the cancer cell membrane and tumor blood vessels. The peptide self-assembled owing to the excellent self-assembling property of "FFG". "FFG" benefited from the closer assembly of AIEgens (MPA-Ph-R-COOH) in the EphA2 cluster; therefore, the luminescent agents AIEgens arranged more compactly, showing a greater fluorescence conversion rate and higher sensitivity. This efficient fluorescent probe is suitable for accurate imaging. AIE dyes also have great potential in bacterial imaging and treatment. Yang et al.¹⁶⁹ proposed a fluorescent probe (TPEPy-Py) for detecting the activity of bacterial ALP. Peptides containing phosphorylated tyrosine could be dephosphorylated by bacterial ALPs. Dephosphorylation increased the hydrophobicity of peptide conjugates, rendering their aggregates to self-assemble into fibrous structures on the bacterial surface, thus initiating AIEgen fluorescence. In addition, Liu et al.⁴⁷ proposed a probe for the diagnosis and treatment of Gram-positive bacterial infections. Vancomycin in AIEgen-peptide conjugate could specifically bind to Gram-positive bacteria, triggering the self-assembly of phenylalanine-phenylalanine (FF) dipeptide, and thus turning on the fluorescence of AIEgen and simultaneously enhancing ROS generation. The integration of AIEgen and SAPs represents a potential strategy for disease diagnosis and treatment.

Smart SAPs for Magnetic Resonance Imaging.

Magnetic resonance imaging (MRI) provides high spatial resolution, good soft tissue imaging effect, and three-dimensional spatial imaging. However, owing to the low sensitivity of MRI, contrast agents are usually used to improve MRI sensitivity to differentiate tumors from normal tissues. MRI contrast agents can be divided into longitudinal relaxation contrast agents (T1 preparation) and transverse relaxation contrast agents (T2 preparation). The applications of the two contrast agents are described below.

The T1 reagent shortens T1 by the direct action of hydrogen nuclei and paramagnetic metal ions in water molecules and has high signal intensity and relatively bright T1-weighted images. T1 is used for observation and anatomy. Accardo et al.¹⁷¹ designed a gadolinium complex-based MRI contrast agent in which the Gd-complex was connected to one end of the PEG₈-(FY)₃ polymer peptide. The peptide self-assembled into crossed β nanostructures in water and formed a soft hydrogel at a concentration above 1.0 wt %, thus increasing the aggregation of signal molecules (Gd³⁺). As a magnetic resonance supramolecular contrast agent, it improved the inherent resolution of diagnostic imaging. Li et al.¹⁴⁵ designed a T1-weighted MRI probe (GFV) based on the strategy of supramolecular self-assembly. The antibiotic molecule vancomycin in the probe targeted against *Staphylococcus aureus*. Owing to $\pi-\pi$ stacking, the self-assembly motif in the probe could be self-assembled into nanoaggregates, and the T1 signal molecule (Gd³⁺) could also be aggregated, providing the probe with a high longitudinal relaxation rate (r_1). This probe could diagnose bacterial infections and monitor therapeutic drugs in real-time.

The T2 reagent shortens T2 by interfering with the heterogeneity of the external local magnetic environment so that the adjacent hydrogen protons quickly generate a diphasic in relaxation. The T2-weighted images are dark and show a low signal intensity. T2 is conducive to the observation of lesions and is sensitive to aqueous tissues. Zhu et al.¹⁷² designed superparamagnetic iron oxide nanoparticles (SPIONs), a self-

assembled peptide coupled with SPION and modified the functional peptide IKVAV to track stem cells. Nanofibers doped with the IKVAV sequence could induce rapid and selective differentiation of neural progenitor cells into neurons. This peptide significantly improved the ability of rat mesenchymal stem cells (MSCs) to attach to the scaffold surface, increased the stability of SPION suspension, and promoted MSCs uptake. Using SPION as a contrast agent for stem cell tracking improved transverse relaxivities (r_2) and MRI efficiency.

The T1/T2 dual-mode MRI contrast agent has a higher relaxation rate in MRI. Wang et al.¹⁷⁰ designed an enzyme-responsive polymer peptide-porphyrin conjugate PPPC containing a hyperbranched polymer backbone, a self-assembled peptide linked with an enzyme-cleavable peptide-poly(ethylene glycol) terminal, a bacterial targeting peptide, and a porphyrin sonosensitizer (MnTCPP) segment. Once the PPPC nanoparticles reached the bacterial infection area where gelatinase was overexpressed, the PEG protective layer was removed, and led to the aggregation of photosensitizer caused by self-assembly. The combined MRI technology of T1 and T2 helped monitor the accumulation of the sonosensitizer porphyrin. Ultrasound was initiated to treat the bacterial infection accurately when the concentration of nanoparticles reached the minimum inhibitory concentration (MIC). This MRI-guided system showed enhanced tissue penetration depth, drug concentration monitoring, induction accumulation of morphological transformation, and improvement of treatment ability for drug-resistant bacteria (Figure 9C).

Smart SAPs for Photoacoustic Imaging. Photoacoustic imaging (PAI) is a noninvasive and nonionizing imaging technology. PAI provides high-resolution and high-sensitivity tissue imaging by combining the high contrast characteristics of optical imaging with the high penetration depth characteristics of ultrasonic imaging.

Several PAI probes have been developed based on NIR dyes (such as ICG, porphyrin, and cyanine). As PAI contrast agents, they provide improved resolution compared to traditional imaging technologies because of the low autofluorescence, deep tissue penetration, and minimal light scattering.¹⁷³ These photosensitizers can also be used in photothermal therapy as they convert light energy into heat to ablate cancer cells. Therefore, such photosensitizers can be used for the integration of imaging and treatment. Liu et al.¹⁷⁴ designed a nanosystem with all-in-one property for tumor PAI and chemo-photothermal combination therapy. Under the stimulation of porphyrin photothermal effect, cancer cells were more susceptible to the chemotherapy drugs of tyrosertavide, giving rise to enhanced histone acetylation and cell apoptosis. In addition, with the help of PA image-guided mild hyperthermia, the tumor inhibition rate of chemotherapy-photothermal combination therapy with a single injection reached to 70%, which could significantly reduce the dose of chemotherapy while imaging.

In addition to the NIR dye-based probe, PAI can also be achieved using responsive precursors. Wang et al.¹⁷⁵ designed a self-assembled nanogel in which SiO₂ nanoparticles were used as an inorganic core. The protonation process was induced by *in situ* amidation, and a self-assembled dilysine coordination iron (Fe(Lys)₂) functionalized polypeptide gel (SiO₂@MCSGs) was constructed on the nanointerface. SiO₂@MCSGs exhibited superoxide dismutase (SOD) and peroxidase (POD) activities. After loading the substrate 2,2'-

azinobis(3-ethylbenzthiazoline-6-sulfonate (ABTS), SiO_2 @MCSGsABTS could transform O_2 in the TME into an H_2O_2 intermediate. Then, it serially catalyzed ABTS oxidation to an oxidation state with strong absorption in the NIR band, making it an ideal PAI contrast agent. The self-assembled nanogel simulant SiO_2 @MCSGsABTS has great potential in the PAI of tumors.

Smart SAPs for Multimodality Imaging. Multimodal imaging combines the advantages of various imaging technologies, overcomes the shortcomings of single imaging technology, and provides more detailed and accurate diagnostic information based on high sensitivity and resolution to improve diagnosis and treatment methods.

Zhang et al.¹⁷⁶ designed a double-targeted double-imaging agent probe (Cy5.5-SAPD-99 mTc) for glioblastoma multiforme treatment. The cyclic heptapeptide comprised an RGD homing motif and a mitochondria-targeting motif, which targeted caspase3-integrin and KLAK pro-apoptotic motifs, respectively, to induce cancer cell apoptosis by producing ROS and activating caspase-3. Simultaneously, the NIR fluorescent dye for optical imaging and the β/γ -emitting radionuclides for SPECT imaging were subjected to the modified cyclic heptapeptide, realizing the bimodal imaging and clinical treatment of glioblastoma multiforme. Bimodal imaging can be used to target tumor sites and blood vessels, thereby benefiting patients with atherosclerosis. Cao et al.¹⁷⁷ designed a nanoprobe to monitor the generation of blood vessels in atherosclerosis through double imaging. They constructed a human serum albumin (HSA) nanoprobe (ICG-HSA-RGDfk NPS, IHR-NPs) by coating indocyanine green (ICG) on RGDfk peptide through electrostatic interaction. HSA was used as a natural drug carrier owing to its inherent biocompatibility. The RGDfk peptide targeted integrin $\alpha_1\beta_3$, with ICG acting as an excellent vascular contrast agent. The *in vivo* lipids were imaged at an excitation wavelength of 1720 nm, thereby performing IVPA/IVUS double imaging of blood vessels resulting from atherosclerosis.

CONCLUSIONS AND PERSPECTIVE

SAPs link multidisciplinary research fields such as chemistry, material science, and life science. The ordered structure of SAPs is the result of cooperation between molecules through noncovalent interactions, including hydrogen bonding, π - π stacking, and electrostatic, hydrophobic, and van der Waals interactions. These noncovalent interactions contribute to the formation of β -sheet, α -helix, or PAs, further promoting higher hierarchical structure, like nanospheres, nanofibers, and nanowires.

Molecularly stimuli-responsive SAPs respond to internal (pH, enzyme, ROS, and temperature) and external (light and magnetism) stimuli. Among the internal stimuli, pH, enzyme, and temperature responses are significantly applied to SAPs and depend on the nature of the peptide itself, whereas ROS-responsive SAPs require the introduction of ROS-cleavable bonds. Light is the most widely used stimulus factor among external stimuli and leads to the development of PDT and PTT therapies. In addition, some researchers have successfully developed SAPs using the highly specific binding characteristics between receptors and ligands. SAPs can be programmed to perform dual or multiple responsive morphological transformations, allowing for targeted imaging and therapy. The morphological transformation of SAPs is the result of reshaping the balance of intra/intermolecular interactions.

Guidelines to SAPs design should be function oriented. SAPs can achieve different functions by introducing different components. Through passive/active targeting, SAPs can be enriched at the target site, thus increasing the cargoes concentration and enhancing therapeutic effect. The responsively converted nanoparticles can expose active sites and improve the cellular internalization of SAPs. While the transformed nanofibers at the target site can prolong retention time, disturb the organelle function, block the receptor–ligand recognition, prevent tumor metastasis, form the ECM, or promote cell growth. SAPs have promising application prospects in antitumor and antibacterial therapies, tissue repair, and imaging.

There are a lot of preclinical and clinical studies on SAPs. EAK16 and RADA16 are the most widely used SAPs for surgery and construction of nanofiber scaffolds for cell repair and regeneration.¹⁷⁸ The SAP RADA16 is sold as a hemostatic agent for surgery (PuraStat) and a reagent for life science research (PuraMatrix). PuraMatrix is sold directly by 3-D Matrix and through distributors including Corning, VWR, Fisher Scientific, and others.¹⁷⁹ Designing from scratch or combining mature SAPs to develop stimuli-responsive SAPs help us obtain the smart therapy/imaging system. At present, there are many effective peptides, but relatively few have been put into clinical use. Smart SAPs can help solve the limited problems. For example, more than 5000 natural and synthetic AMPs have been discovered, while only eight have been approved by the Food and Drug Administration (FDA).¹⁸⁰ Incorporating AMPs into smart SAPs can help solve the problems of poor stability and side effects *in vivo*. Some smart SAPs are in clinical trials. For example, P11-4 (Ac-QQRFEWEFEQQ-NH₂) can be self-assembled into β -sheet amyloids with a hydrogel appearance at low pH, which is used for biomimetic mineralization, enamel regeneration, and oral care agent.¹⁸¹

Although SAP research has advanced considerably, emerging challenges must be addressed including (i) some undesired morphological transformation out of the target sites caused by the complex internal environment; (ii) lack of mature methods and tools for real-time feedback *in vivo* self-assembly processes; and (iii) application of SAP in tissues or organs which lack specific stimuli like the overexpressed enzymes, the low pH, and so on. To sum up, a more sophisticated design must be applied to realize adaptive self-assembly *in vivo* and precise superstructure control. Tools and methods must be developed to characterize and accurately control the dynamic behavior of self-assembly. More specific stimulus-response mechanisms must be developed to improve safety and response efficiency. It is necessary to develop methods that can achieve enrichment and morphological transformation in conditions lacking specific stimuli, and the ligand–receptor/cytokine responsive SAP is a promising option. In the future, smart SAPs can be developed by learning from nature and benefit the natural society.

AUTHOR INFORMATION

Corresponding Authors

Nicole F. Steinmetz – Department of NanoEngineering, Department of Bioengineering, Department of Radiology, Moores Cancer Center, Center for Nano-ImmunoEngineering, Center for Engineering in Cancer, Institute for Materials Discovery and Design, University of California, San Diego, La

Jolla, California 92093, United States;  orcid.org/0000-0002-0130-0481; Email: nsteinmetz@ucsd.edu

Hui Cai – School of Pharmaceutical Sciences (Shenzhen), Shenzhen Campus of Sun Yat-Sen University, Shenzhen 518107, China;  orcid.org/0000-0002-5394-8167; Email: caihui5@mail.sysu.edu.cn

Authors

Yang Zhou – School of Pharmaceutical Sciences (Shenzhen), Shenzhen Campus of Sun Yat-Sen University, Shenzhen 518107, China

Qianqian Li – School of Pharmaceutical Sciences (Shenzhen), Shenzhen Campus of Sun Yat-Sen University, Shenzhen 518107, China; Shenzhen Bay Laboratory, Shenzhen 518055, China

Ye Wu – School of Pharmaceutical Sciences (Shenzhen), Shenzhen Campus of Sun Yat-Sen University, Shenzhen 518107, China

Xinyu Li – School of Pharmaceutical Sciences (Shenzhen), Shenzhen Campus of Sun Yat-Sen University, Shenzhen 518107, China

Ya Zhou – School of Pharmaceutical Sciences (Shenzhen), Shenzhen Campus of Sun Yat-Sen University, Shenzhen 518107, China

Zhu Wang – Department of Urology, Affiliated People's Hospital of Longhua Shenzhen, Southern Medical University, Shenzhen, Guangdong 518109, PR China

Hui Liang – Department of Urology, Affiliated People's Hospital of Longhua Shenzhen, Southern Medical University, Shenzhen, Guangdong 518109, PR China

Feiqing Ding – School of Pharmaceutical Sciences (Shenzhen), Shenzhen Campus of Sun Yat-Sen University, Shenzhen 518107, China;  orcid.org/0000-0002-0211-7101

Sheng Hong – School of Pharmaceutical Sciences (Shenzhen), Shenzhen Campus of Sun Yat-Sen University, Shenzhen 518107, China

Complete contact information is available at:
<https://pubs.acs.org/10.1021/acsnano.3c01452>

Author Contributions

#Y.Z. and Q.L. contributed equally to this work.

Notes

The authors declare no competing financial interest.

ACKNOWLEDGMENTS

This work was supported partly by the Shenzhen Science and Technology Program (no. JCYJ20220818102005011 to H.C.), National Natural Science Foundation of China (no. 22277150 to H.C.; no. 22007106 to Q.L.), the “Pearl River Talent Plan” Innovation and Entrepreneurship Team Project of Guangdong Province (no. 2021ZT09Y544 to H.C.), the Fundamental Research Funds for the Central Universities (no. 22lgj10 to H.C.; no. 31610011 to F.D.), the Province Natural Science Fund of Guangdong (no. 2022A1515011109 to H.C.; no. 42030015 to F.D.), and supported in part by the UC San Diego Materials Research Science and Engineering Center (UCSD MRSEC) funded by the National Science Foundation (Grant DMR-2011924). Thanks to Figdraw (www.figdraw.com) for providing some elements for Scheme 1.

VOCABULARY

Self-assembly, technology of spontaneous formation of ordered structure by basic structural units; nanoparticle, ultrafine unit with dimensions measured in nanometers; target delivery, technology for transporting cargoes to the target area through nanocarriers; tumor microenvironment, a comprehensive system mainly composed of tumor cells, the surrounding immune and inflammatory cells, tumor-related fibroblasts, and nearby interstitial tissue, microvessels as well as various cytokines and chemokines; imaging, the process of forming images that represent things such as sound waves, temperature, chemicals, or electrical activity

REFERENCES

- (1) Liang, Y.; Xie, Y.; Chen, D.; Guo, C.; Hou, S.; Wen, T.; Yang, F.; Deng, K.; Wu, X.; Smalyukh, I. I.; Liu, Q. Symmetry Control of Nanorod Superlattice Sriven by a Governing Force. *Nat. Commun.* **2017**, *8*, 1410.
- (2) Léger, P.; Nachman, E.; Richter, K.; Tamietti, C.; Koch, J.; Burk, R.; Kummer, S.; Xin, Q.; Stanifer, M.; Bouloy, M.; Boulant, S.; Kräusslich, H.-G.; Montagutelli, X.; Flamand, M.; Nussbaum-Krammer, C.; Lozach, P.-Y. NSs Amyloid Formation Is Associated with the Virulence of Rift Valley Fever Virus in Mice. *Nat. Commun.* **2020**, *11*, 3281.
- (3) Wang, J.; Liu, K.; Xing, R.; Yan, X. Peptide Self-Assembly: Thermodynamics and Kinetics. *Chem. Soc. Rev.* **2016**, *45*, 5589–5604.
- (4) Vaissière, A.; Aldrian, G.; Konate, K.; Lindberg, M. F.; Jourdan, C.; Telmar, A.; Seisel, Q.; Fernandez, F.; Viguier, V.; Genevois, C.; Couillaud, F.; Boisguerin, P.; Deshayes, S. A *Retro-Inverso* Cell-Penetrating Peptide for siRNA Delivery. *J. Nanobiotechnology*. **2017**, *15*, 34.
- (5) Zhao, X. X.; Li, L. L.; Zhao, Y.; An, H. W.; Cai, Q.; Lang, J. Y.; Han, X. X.; Peng, B.; Fei, Y.; Liu, H.; Qin, H.; Nie, G.; Wang, H. *In situ* Self-Assembled Nanofibers Precisely Target Cancer-Associated Fibroblasts for Improved Tumor Imaging. *Angew. Chem., Int. Ed. Engl.* **2019**, *58*, 15287–15294.
- (6) Chairatana, P.; Nolan, E. M. Human α -Defensin 6: a Small Peptide That Self-Assembles and Protects the Host by Entangling Microbes. *Acc. Chem. Res.* **2017**, *50*, 960–967.
- (7) Lopez-Silva, T. L.; Cristobal, C. D.; Edwin Lai, C. S.; Leyva-Aranda, V.; Lee, H. K.; Hartgerink, J. D. Self-Assembling Multidomain Peptide Hydrogels Accelerate Peripheral Nerve Regeneration after Crush Injury. *Biomaterials* **2021**, *265*, 120401.
- (8) Acar, H.; Ting, J. M.; Srivastava, S.; LaBelle, J. L.; Tirrell, M. V. Molecular Engineering Solutions for Therapeutic Peptide Delivery. *Chem. Soc. Rev.* **2017**, *46*, 6553–6569.
- (9) Moore, A. N.; Hartgerink, J. D. Self-Assembling Multidomain Peptide Nanofibers for Delivery of Bioactive Molecules and Tissue Regeneration. *Acc. Chem. Res.* **2017**, *50*, 714–722.
- (10) Qi, G. B.; Gao, Y. J.; Wang, L.; Wang, H. Self-Assembled Peptide-Based Nanomaterials for Biomedical Imaging and Therapy. *Adv. Mater.* **2018**, *30*, No. e1703444.
- (11) Wang, H.; Feng, Z.; Xu, B. Assemblies of Peptides in a Complex Environment and Their Applications. *Angew. Chem., Int. Ed. Engl.* **2019**, *58*, 10423–10432.
- (12) Yi, Y.; Yu, M.; Li, W.; Zhu, D.; Mei, L.; Ou, M. Vaccine-Like Nanomedicine for Cancer Immunotherapy. *J. Controlled Release* **2023**, *355*, 760–778.
- (13) Zeng, W.; Zhang, H.; Deng, Y.; Jiang, A.; Bao, X.; Guo, M.; Li, Z.; Wu, M.; Ji, X.; Zeng, X.; Mei, L. Dual-Response Oxygen-Generating MnO_2 Nanoparticles with Polydopamine Modification for Combined Photothermal-Photodynamic Therapy. *Chem. Eng. J.* **2020**, *389*, 124494.
- (14) Zeng, X.; Liu, G.; Tao, W.; Ma, Y.; Zhang, X.; He, F.; Pan, J.; Mei, L.; Pan, G. A Drug-Self-Gated Mesoporous Antitumor Nanoplatform Based on pH-Sensitive Dynamic Covalent Bond. *Adv. Funct. Mater.* **2017**, *27*, 1605985.

(15) Sheng, S.; Yu, X.; Xing, G.; Jin, L.; Zhang, Y.; Zhu, D.; Dong, X.; Mei, L.; Lv, F. An Apoptotic Body-Based Vehicle with Navigation for Photothermal-Immunotherapy by Precise Delivery and Tumor Microenvironment Regulation. *Adv. Funct. Mater.* **2023**, *33*, 2212118.

(16) Li, Q.; Shi, Z.; Ou, M.; Li, Z.; Luo, M.; Wu, M.; Dong, X.; Lu, L.; Lv, F.; Zhang, F.; Mei, L. pH-Labile Artificial Natural Killer Cells for Overcoming Tumor Drug Resistance. *J. Controlled Release* **2022**, *352*, 450–458.

(17) Tao, W.; Zhu, X.; Yu, X.; Zeng, X.; Xiao, Q.; Zhang, X.; Ji, X.; Wang, X.; Shi, J.; Zhang, H.; Mei, L. Black Phosphorus Nanosheets as a Robust Delivery Platform for Cancer Theranostics. *Adv. Mater.* **2017**, *29*, 10.

(18) Ou, M.; Lin, C.; Wang, Y.; Lu, Y.; Wang, W.; Li, Z.; Zeng, W.; Zeng, X.; Ji, X.; Mei, L. Heterojunction Engineered Bioactive Chlorella for Cascade Promoted Cancer Therapy. *J. Controlled Release* **2022**, *345*, 755–769.

(19) Zhang, Z.; Ai, S.; Yang, Z.; Li, X. Peptide-Based Supramolecular Hydrogels for Local Drug Delivery. *Adv. Drug. Delivery Rev.* **2021**, *174*, 482–503.

(20) Jiang, Q.; Liu, X.; Liang, G.; Sun, X. Self-Assembly of Peptide Nanofibers for Imaging Applications. *Nanoscale* **2021**, *13*, 15142–15150.

(21) Ma, W.; Sha, S. N.; Chen, P. L.; Yu, M.; Chen, J. J.; Huang, C. B.; Yu, B.; Liu, Y.; Liu, L. H.; Yu, Z. Q. A Cell Membrane-Targeting Self-Delivery Chimeric Peptide for Enhanced Photodynamic Therapy and *in situ* Therapeutic Feedback. *Adv. Healthc. Mater.* **2020**, *9*, No. e1901100.

(22) De Santis, E.; Ryadnov, M. G. Peptide Self-Assembly for Nanomaterials: the Old New Kid on the Block. *Chem. Soc. Rev.* **2015**, *44*, 8288–300.

(23) Karimi, M.; Ghasemi, A.; Sahandi Zangabad, P.; Rahighi, R.; Moosavi Basri, S. M.; Mirshekari, H.; Amiri, M.; Shafaei Pishabad, Z.; Aslani, A.; Bozorgomid, M.; Ghosh, D.; Beyzavi, A.; Vaseghi, A.; Aref, A. R.; Haghani, L.; Bahrami, S.; Hamblin, M. R. Smart Micro/Nanoparticles in Stimulus-Responsive Drug/Gene Delivery Systems. *Chem. Soc. Rev.* **2016**, *45*, 1457–501.

(24) Rudra, J. S.; Tian, Y. F.; Jung, J. P.; Collier, J. H. A Self-Assembling Peptide Acting as an Immune Adjuvant. *Proc. Natl. Acad. Sci. U. S. A.* **2010**, *107*, 622–627.

(25) Huang, Z. H.; Shi, L.; Ma, J. W.; Sun, Z. Y.; Cai, H.; Chen, Y. X.; Zhao, Y. F.; Li, Y. M. A Totally Synthetic, Self-Assembling, Adjuvant-Free MUC1 Glycopeptide Vaccine for Cancer Therapy. *J. Am. Chem. Soc.* **2012**, *134*, 8730–8733.

(26) Chen, J.; Zou, X. Self-Assemble Peptide Biomaterials and Their Biomedical Applications. *Bioact. Mater.* **2019**, *4*, 120–131.

(27) Zhang, S.; Holmes, T.; Lockshin, C.; Rich, A. Spontaneous Assembly of a Self-Complementary Oligopeptide to Form a Stable Macroscopic Membrane. *Proc. Natl. Acad. Sci. U. S. A.* **1993**, *90*, 3334–8.

(28) Freibaum, B. D.; Taylor, J. P. The Role of Dipeptide Repeats in C9ORF72-Related ALS-FTD. *Front. Mol. Neurosci.* **2017**, *10*, 35.

(29) Schneider, J. P.; Pochan, D. J.; Ozbas, B.; Rajagopal, K.; Pakstis, L.; Kretsinger, J. Responsive Hydrogels from the Intramolecular Folding and Self-Assembly of a Designed Peptide. *J. Am. Chem. Soc.* **2002**, *124*, 15030–15037.

(30) Kretsinger, J. K.; Haines, L. A.; Ozbas, B.; Pochan, D. J.; Schneider, J. P. Cytocompatibility of Self-Assembled β -Hairpin Peptide Hydrogel Surfaces. *Biomaterials* **2005**, *26*, 5177–86.

(31) Kim, S.; Kim, J. H.; Lee, J. S.; Park, C. B. Beta-Sheet-Forming, Self-Assembled Peptide Nanomaterials Towards Optical, Energy, and Healthcare Applications. *Small* **2015**, *11*, 3623–3640.

(32) Stefani, M.; Dobson, C. M. Protein Aggregation and Aggregate Toxicity: New Insights into Protein Folding, Misfolding Diseases and Biological Evolution. *J. Mol. Med.* **2003**, *81*, 678–699.

(33) Caughey, B.; Lansbury, P. T. Protofibrils, Pores, Fibrils, and Neurodegeneration: Separating the Responsible Protein Aggregates from the Innocent Bystanders. *Annu. Rev. Neurosci.* **2003**, *26*, 267–298.

(34) Nagai, Y.; Inui, T.; Popiel, H. A.; Fujikake, N.; Hasegawa, K.; Urade, Y.; Goto, Y.; Naiki, H.; Toda, T. A Toxic Monomeric Conformer of the Polyglutamine Protein. *Nat. Struct. Mol. Biol.* **2007**, *14*, 332–340.

(35) Lapenta, F.; Aupic, J.; Strmsek, Z.; Jerala, R. Coiled Coil Protein Origami: from Modular Design Principles Towards Biotechnological Applications. *Chem. Soc. Rev.* **2018**, *47*, 3530–3542.

(36) Bera, S.; Mondal, S.; Xue, B.; Shimon, L. J. W.; Cao, Y.; Gazit, E. Rigid Helical-Like Assemblies from a Self-Aggregating Tripeptide. *Nat. Mater.* **2019**, *18*, 503–509.

(37) Pandya, M. J.; Spooner, G. M.; Sunde, M.; Thorpe, J. R.; Rodger, A.; Woolfson, D. N. Sticky-End Assembly of a Designed Peptide Fiber Provides Insight into Protein Fibrillogenesis. *Biochemistry* **2000**, *39*, 8728–34.

(38) Papapostolou, D.; Smith, A. M.; Atkins, E. D. T.; Oliver, S. J.; Ryadnov, M. G.; Serpell, L. C.; Woolfson, D. N. Engineering Nanoscale Order into a Designed Protein Fiber. *Proc. Natl. Acad. Sci. U. S. A.* **2007**, *104*, 10853–10858.

(39) Fletcher, J. M.; Harniman, R. L.; Barnes, F. R. H.; Boyle, A. L.; Collins, A.; Mantell, J.; Sharp, T. H.; Antognazzi, M.; Booth, P. J.; Linden, N.; Miles, M. J.; Sessions, R. B.; Verkade, P.; Woolfson, D. N. Self-Assembling Cages from Coiled-Coil Peptide Modules. *Science* **2013**, *340*, 595–9.

(40) Dasgupta, A.; Das, D. Designer Peptide Amphiphiles: Self-Assembly to Applications. *Langmuir* **2019**, *35*, 10704–10724.

(41) Hartgerink, J. D.; Beniash, E.; Stupp, S. I. Self-Assembly and Mineralization of Peptide-Amphiphile Nanofibers. *Science* **2001**, *294*, 1684–1688.

(42) Versluis, F.; Tomatsu, I.; Kehr, S.; Fregonese, C.; Tepper, A.; Stuart, M. C. A.; Ravoo, B. J.; Koning, R. I.; Kros, A. Shape and Release Control of a Peptide Decorated Vesicle Through pH Sensitive Orthogonal Supramolecular Interactions. *J. Am. Chem. Soc.* **2009**, *131*, 13186–13187.

(43) Jiao, D. Z.; Geng, J.; Loh, X. J.; Das, D.; Lee, T. C.; Scherman, O. A. Supramolecular Peptide Amphiphile Vesicles Through Host-Guest Complexation. *Angew. Chem., Int. Ed. Engl.* **2012**, *51*, 9633–9637.

(44) Delfi, M.; Sartorius, R.; Ashrafizadeh, M.; Sharifi, E.; Zhang, Y.; De Berardinis, P.; Zarrabi, A.; Varma, R. S.; Tay, F. R.; Smith, B. R.; Makvandi, P. Self-Assembled Peptide and Protein Nanostructures for Anti-Cancer Therapy: Targeted Delivery, Stimuli-Responsive Devices and Immunotherapy. *Nano Today* **2021**, *38*, 101119.

(45) Cai, W.; Wang, J.; Chu, C.; Chen, W.; Wu, C.; Liu, G. Metal-Organic Framework-Based Stimuli-Responsive Systems for Drug Delivery. *Adv. Sci. (Weinh)* **2019**, *6*, 1801526.

(46) Song, Z.; Chen, X.; You, X.; Huang, K.; Dhinakar, A.; Gu, Z.; Wu, J. Self-Assembly of Peptide Amphiphiles for Drug Delivery: the Role of Peptide Primary and Secondary Structures. *Biomater. Sci.* **2017**, *5*, 2369–2380.

(47) Yang, C.; Hu, F.; Zhang, X.; Ren, C.; Huang, F.; Liu, J.; Zhang, Y.; Yang, L.; Gao, Y.; Liu, B.; Liu, J. Combating Bacterial Infection by *in situ* Self-Assembly of AIEgen-Peptide Conjugate. *Biomaterials* **2020**, *244*, 119972.

(48) Ruan, L.; Chen, W.; Wang, R.; Lu, J.; Zink, J. I. Magnetically Stimulated Drug Release Using Nanoparticles Capped by Self-Assembling Peptides. *ACS Appl. Mater. Interfaces* **2019**, *11*, 43835–43842.

(49) He, L.; Xiao, Q.; Zhao, Y.; Li, J.; Reddy, S.; Shi, X.; Su, X.; Chiu, K.; Ramakrishna, S. Engineering an Injectable Electroactive Nanohybrid Hydrogel for Boosting Peripheral Nerve Growth and Myelination in Combination with Electrical Stimulation. *ACS Appl. Mater. Interfaces* **2020**, *12*, 53150–53163.

(50) Gao, J.; Zhan, J.; Yang, Z. Enzyme-Instructed Self-Assembly (EISA) and Hydrogelation of Peptides. *Adv. Mater.* **2020**, *32*, No. e1805798.

(51) Zhang, C.; Shafi, R.; Lampel, A.; MacPherson, D.; Pappas, C. G.; Narang, V.; Wang, T.; Maldarelli, C.; Ulijn, R. V. Switchable Hydrolase Based on Reversible Formation of Supramolecular

Catalytic Site Using a Self-Assembling Peptide. *Angew. Chem., Int. Ed. Engl.* **2017**, *56*, 14511–14515.

(52) Wang, J.; Dzuricky, M.; Chilkoti, A. The Weak Link: Optimization of the Ligand-Nanoparticle Interface to Enhance Cancer Cell Targeting by Polymer Micelles. *Nano Lett.* **2017**, *17*, 5995–6005.

(53) Sun, B.; Tao, K.; Jia, Y.; Yan, X.; Zou, Q.; Gazit, E.; Li, J. Photoactive Properties of Supramolecular Assembled Short Peptides. *Chem. Soc. Rev.* **2019**, *48*, 4387–4400.

(54) Cheng, K.; Ding, Y.; Zhao, Y.; Ye, S.; Zhao, X.; Zhang, Y.; Ji, T.; Wu, H.; Wang, B.; Anderson, G. J.; Ren, L.; Nie, G. Sequentially Responsive Therapeutic Peptide Assembling Nanoparticles for Dual-Targeted Cancer Immunotherapy. *Nano Lett.* **2018**, *18*, 3250–3258.

(55) Jiang, X.; Fan, X.; Zhang, R.; Xu, W.; Wu, H.; Zhao, F.; Xiao, H.; Zhang, C.; Zhao, C.; Wu, G. *In situ* Tumor-Triggered Subcellular Precise Delivery of Multi-Drugs for Enhanced Chemo-Photothermal-Starvation Combination Antitumor Therapy. *Theranostics* **2020**, *10*, 12158–12173.

(56) Dou, X. Q.; Feng, C. L. Amino Acids and Peptide-Based Supramolecular Hydrogels for Three-Dimensional Cell Culture. *Adv. Mater.* **2017**, *29*, 1604062.

(57) Aggeli, A.; Bell, M.; Carrick, L. M.; Fishwick, C. W.; Harding, R.; Mawer, P. J.; Radford, S. E.; Strong, A. E.; Boden, N. pH as a Trigger of Peptide Beta-Sheet Self-Assembly and Reversible Switching Between Nematic and Isotropic phases. *J. Am. Chem. Soc.* **2003**, *125*, 9619–28.

(58) Han, K.; Zhang, J.; Zhang, W.; Wang, S.; Xu, L.; Zhang, C.; Zhang, X.; Han, H. Tumor-Triggered Geometrical Shape Switch of Chimeric Peptide for Enhanced *in vivo* Tumor Internalization and Photodynamic Therapy. *ACS Nano* **2017**, *11*, 3178–3188.

(59) Ye, B.; Wang, Q.; Hu, H.; Shen, Y.; Fan, C.; Chen, P.; Ma, Y.; Wu, H.; Xiang, M. Restoring Autophagic Flux Attenuates Cochlear Spiral Ganglion Neuron Degeneration by Promoting TFEB Nuclear Translocation *via* Inhibiting MTOR. *Autophagy* **2019**, *15*, 998–1016.

(60) Sun, B.; Chang, R.; Cao, S.; Yuan, C.; Zhao, L.; Yang, H.; Li, J.; Yan, X.; Hest, J. C. M. Acid-Activatable Transmorphic Peptide-Based Nanomaterials for Photodynamic Therapy. *Angew. Chem., Int. Ed. Engl.* **2020**, *59*, 20582–20588.

(61) Jin, C.; Li, G.; Wu, X.; Liu, J.; Wu, W.; Chen, Y.; Sasaki, T.; Chao, H.; Zhang, Y. Robust Packing of a Self-Assembling Iridium Complex *via* Endocytic Trafficking for Long-Term Lysosome Tracking. *Angew. Chem., Int. Ed. Engl.* **2021**, *60*, 7597–7601.

(62) Xu, L.; Wang, Y.; Zhu, C.; Ren, S.; Shao, Y.; Wu, L.; Li, W.; Jia, X.; Hu, R.; Chen, R.; Chen, Z. Morphological Transformation Enhances Tumor Retention by Regulating the Self-Assembly of Doxorubicin-Peptide Conjugates. *Theranostics* **2020**, *10*, 8162–8178.

(63) Kumar, M.; Son, J.; Huang, R. H.; Sementa, D.; Lee, M.; O'Brien, S.; Ulijn, R. V. *In situ*, Noncovalent Labeling and Stimulated Emission Depletion-Based Super-Resolution Imaging of Supramolecular Peptide Nanostructures. *ACS Nano* **2020**, *14*, 15056–15063.

(64) Zhan, J.; Cai, Y.; He, S.; Wang, L.; Yang, Z. Tandem Molecular Self-Assembly in Liver Cancer Cells. *Angew. Chem., Int. Ed. Engl.* **2018**, *57*, 1813–1816.

(65) Zhou, J.; Du, X.; Berciu, C.; Del Signore, S. J.; Chen, X.; Yamagata, N.; Rodal, A. A.; Nicastro, D.; Xu, B. Cellular Uptake of a Taurine-Modified, Ester Bond-Decorated D-Peptide Derivative *via* Dynamin-Based Endocytosis and Macropinocytosis. *Mol. Ther.* **2018**, *26*, 648–658.

(66) He, H.; Lin, X.; Guo, J.; Wang, J.; Xu, B. Perimitochondrial Enzymatic Self-Assembly for Selective Targeting the Mitochondria of Cancer Cells. *ACS Nano* **2020**, *14*, 6947–6955.

(67) Cheng, D. B.; Zhang, X. H.; Gao, Y. J.; Wang, D.; Wang, L.; Chen, H.; Qiao, Z. Y.; Wang, H. Site-Specific Construction of Long-Term Drug Depot for Suppression of Tumor Recurrence. *Small* **2019**, *15*, No. e1901813.

(68) Li, L. L.; Ma, H. L.; Qi, G. B.; Zhang, D.; Yu, F.; Hu, Z.; Wang, H. Pathological-Condition-Driven Construction of Supramolecular Nanoassemblies for Bacterial Infection Detection. *Adv. Mater.* **2016**, *28*, 254–62.

(69) An, H. W.; Li, L. L.; Wang, Y.; Wang, Z.; Hou, D.; Lin, Y. X.; Qiao, S. L.; Wang, M. D.; Yang, C.; Cong, Y.; Ma, Y.; Zhao, X. X.; Cai, Q.; Chen, W. T.; Lu, C. Q.; Xu, W.; Wang, H.; Zhao, Y. A Tumour-Selective Cascade Activatable Self-Detained System for Drug Delivery and Cancer Imaging. *Nat. Commun.* **2019**, *10*, 4861.

(70) Li, J.; Shi, J.; Medina, J. E.; Zhou, J.; Du, X.; Wang, H.; Yang, C.; Liu, J.; Yang, Z.; Dinulescu, D. M.; Xu, B. Selectively Inducing Cancer Cell Death by Intracellular Enzyme-Instructed Self-Assembly (EISA) of Dipeptide Derivatives. *Adv. Healthc. Mater.* **2017**, *6*, 1601400.

(71) He, H.; Wang, J.; Wang, H.; Zhou, N.; Yang, D.; Green, D. R.; Xu, B. Enzymatic Cleavage of Branched Peptides for Targeting Mitochondria. *J. Am. Chem. Soc.* **2018**, *140*, 1215–1218.

(72) Tan, W.; Zhang, Q.; Wang, J.; Yi, M.; He, H.; Xu, B. Enzymatic Assemblies of Thiophosphopeptides Instantly Target Golgi Apparatus and Selectively Kill Cancer Cells*. *Angew. Chem., Int. Ed. Engl.* **2021**, *60*, 12796–12801.

(73) Feng, Z.; Wang, H.; Chen, X.; Xu, B. Self-Assembling Ability Determines the Activity of Enzyme-Instructed Self-Assembly for Inhibiting Cancer Cells. *J. Am. Chem. Soc.* **2017**, *139*, 15377–15384.

(74) Adamiak, L.; Touve, M. A.; LeGuyader, C. L. M.; Gianneschi, N. C. Peptide Brush Polymers and Nanoparticles with Enzyme-Regulated Structure and Charge for Inducing or Evading Macrophage Cell Uptake. *ACS Nano* **2017**, *11*, 9877–9888.

(75) Son, J.; Kalafatovic, D.; Kumar, M.; Yoo, B.; Cornejo, M. A.; Contel, M.; Ulijn, R. V. Customizing Morphology, Size, and Response Kinetics of Matrix Metalloproteinase-Responsive Nanostructures by Systematic Peptide Design. *ACS Nano* **2019**, *13*, 1555–1562.

(76) An, H. W.; Hou, D.; Zheng, R.; Wang, M. D.; Zeng, X. Z.; Xiao, W. Y.; Yan, T. D.; Wang, J. Q.; Zhao, C. H.; Cheng, L. M.; Zhang, J. M.; Wang, L.; Wang, Z. Q.; Wang, H.; Xu, W. A Near-Infrared Peptide Probe with Tumor-Specific Excretion-Retarded Effect for Image-Guided Surgery of Renal Cell Carcinoma. *ACS Nano* **2020**, *14*, 927–936.

(77) Judd, J.; Ho, M. L.; Tiwari, A.; Gomez, E. J.; Dempsey, C.; Van Vliet, K.; Igoshin, O. A.; Silberg, J. J.; Agbandje-McKenna, M.; Suh, J. Tunable Protease-Activatable Virus Nanonodes. *ACS Nano* **2014**, *8*, 4740–4746.

(78) Cheng, D. B.; Wang, D.; Gao, Y. J.; Wang, L.; Qiao, Z. Y.; Wang, H. Autocatalytic Morphology Transformation Platform for Targeted Drug Accumulation. *J. Am. Chem. Soc.* **2019**, *141*, 4406–4411.

(79) Olson, O. C.; Joyce, J. A. Cysteine Cathepsin Proteases: Regulators of Cancer Progression and Therapeutic Response. *Nat. Rev. Cancer* **2015**, *15*, 712–29.

(80) Zhang, C.; Liu, L. H.; Qiu, W. X.; Zhang, Y. H.; Song, W.; Zhang, L.; Wang, S. B.; Zhang, X. Z. A Transformable Chimeric Peptide for Cell Encapsulation to Overcome Multidrug Resistance. *Small* **2018**, *14*, No. e1703321.

(81) Li, J.; Ge, Z.; Toh, K.; Liu, X.; Dirisala, A.; Ke, W.; Wen, P.; Zhou, H.; Wang, Z.; Xiao, S.; Van Guyse, J. F. R.; Tockary, T. A.; Xie, J.; Gonzalez-Carter, D.; Kinoh, H.; Uchida, S.; Anraku, Y.; Kataoka, K. Enzymatically Transformable Polymersome-Based Nanotherapeutics to Eliminate Minimal Relapsable Cancer. *Adv. Mater.* **2021**, *33*, No. e2105254.

(82) Yang, L.; Peltier, R.; Zhang, M.; Song, D.; Huang, H.; Chen, G.; Chen, Y.; Zhou, F.; Hao, Q.; Bian, L.; He, M. L.; Wang, Z.; Hu, Y.; Sun, H. Desuccinylation-Triggered Peptide Self-Assembly: Live Cell Imaging of SIRT5 Activity and Mitochondrial Activity Modulation. *J. Am. Chem. Soc.* **2020**, *142*, 18150–18159.

(83) Guo, R. C.; Zhang, X. H.; Fan, P. S.; Song, B. L.; Li, Z. X.; Duan, Z. Y.; Qiao, Z. Y.; Wang, H. *In vivo* Self-Assembly Induced Cell Membrane Phase Separation for Improved Peptide Drug Internalization. *Angew. Chem., Int. Ed. Engl.* **2021**, *60*, 25128–25134.

(84) Sun, M.; Wang, C.; Lv, M.; Fan, Z.; Du, J. Intracellular Self-Assembly of Peptides to Induce Apoptosis Against Drug-Resistant Melanoma. *J. Am. Chem. Soc.* **2022**, *144*, 7337–7345.

(85) Pei, P.; Chen, L.; Fan, R.; Zhou, X. R.; Feng, S.; Liu, H.; Guo, Q.; Yin, H.; Zhang, Q.; Sun, F.; Peng, L.; Wei, P.; He, C.; Qiao, R.; Wang, Z.; Luo, S. Z. Computer-Aided Design of Lasso-Like Self-Assembling Anticancer Peptides with Multiple Functions for Targeted Self-Delivery and Cancer Treatments. *ACS Nano* **2022**, *16*, 13783–13799.

(86) Trachootham, D.; Zhang, H.; Zhang, W.; Feng, L.; Du, M.; Zhou, Y.; Chen, Z.; Pelicano, H.; Plunkett, W.; Wierda, W. G.; Keating, M. J.; Huang, P. Effective Elimination of Fludarabine-Resistant CLL Cells by PEITC Through a Redox-Mediated Mechanism. *Blood* **2008**, *112*, 1912–22.

(87) Liu, L.; Zhang, K.; Sandoval, H.; Yamamoto, S.; Jaiswal, M.; Sanz, E.; Li, Z.; Hui, J.; Graham, B. H.; Quintana, A.; Bellen, H. J. Glial Lipid Droplets and ROS Induced by Mitochondrial Defects Promote Neurodegeneration. *Cell* **2015**, *160*, 177–90.

(88) Cheng, D. B.; Zhang, X. H.; Gao, Y. J.; Ji, L.; Hou, D.; Wang, Z.; Xu, W.; Qiao, Z. Y.; Wang, H. Endogenous Reactive Oxygen Species-Triggered Morphology Transformation for Enhanced Cooperative Interaction with Mitochondria. *J. Am. Chem. Soc.* **2019**, *141*, 7235–7239.

(89) Chen, W.; Li, S.; Lang, J. C.; Chang, Y.; Pan, Z.; Kroll, P.; Sun, X.; Tang, L.; Dong, H. Combined Tumor Environment Triggered Self-Assembling Peptide Nanofibers and Inducible Multivalent Ligand Display for Cancer Cell Targeting with Enhanced Sensitivity and Specificity. *Small* **2020**, *16*, No. e2002780.

(90) Basheer, A.; Shahid, S.; Kang, M. J.; Lee, J. H.; Lee, J. S.; Lim, D. W. Switchable Self-Assembly of Elastin- and Resilin-Based Block Copolypeptides with Converse Phase Transition Behaviors. *ACS Appl. Mater. Interfaces* **2021**, *13*, 24385–24400.

(91) Song, N.; Zhou, Z.; Song, Y.; Li, M.; Yu, X.; Hu, B.; Yu, Z. *In situ* Oxidation-Regulated Self-Assembly of Peptides into Transformable Scaffolds for Cascade Therapy. *Nano Today* **2021**, *38*, 101198.

(92) Wang, M. D.; Lv, G. T.; An, H. W.; Zhang, N. Y.; Wang, H. *In situ* Self-Assembly of Bispecific Peptide for Cancer Immunotherapy. *Angew. Chem., Int. Ed. Engl.* **2022**, *61*, No. e202113649.

(93) Gonzalez-Valdivieso, J.; Girotti, A.; Munoz, R.; Rodriguez-Cabello, J. C.; Arias, F. J. Self-Assembling ELR-Based Nanoparticles as Smart Drug-Delivery Systems Modulating Cellular Growth *via* Akt. *Biomacromolecules* **2019**, *20*, 1996–2007.

(94) Sun, Y.; Ding, F. Thermo- and pH-Responsive Fibrillization of Squid Suckerin A1H1 Peptide. *Nanoscale* **2020**, *12*, 6307–6317.

(95) Zhao, C.; Ma, Z.; Zhu, X. X. Rational Design of Thermoresponsive Polymers in Aqueous Solutions: a Thermodynamics Map. *Prog. Polym. Sci.* **2019**, *90*, 269–291.

(96) Choi, J. W.; Choi, S. H.; Won, J. I. Self-Assembly Behavior of Elastin-Like Polypeptide Diblock Copolymers Containing a Charged Moiety. *Biomacromolecules* **2021**, *22*, 2604–2613.

(97) Sun, S.; Liang, H. W.; Wang, H.; Zou, Q. Light-Triggered Self-Assembly of Peptide Nanoparticles into Nanofibers in Living Cells Through Molecular Conformation Changes and H-Bond Interactions. *ACS Nano* **2022**, *16*, 18978–18989.

(98) Sharma, P.; Kaur, H.; Roy, S. Inducing Differential Self-Assembling Behavior in Ultrashort Peptide Hydrogelators Using Simple Metal Salts. *Biomacromolecules* **2019**, *20*, 2610–2624.

(99) Sahoo, J. K.; VandenBerg, M. A.; Webber, M. J. Kinetic Evolution in Metal-Dependent Self-Assembly of Peptide-Terpyridine Conjugates. *Macromol. Rapid Commun.* **2020**, *41*, No. e1900565.

(100) Wang, A.; Cui, L.; Debnath, S.; Dong, Q.; Yan, X.; Zhang, X.; Ulijn, R. V.; Bai, S. Tuning Supramolecular Structure and Functions of Peptide Bola-Amphiphile by Solvent Evaporation-Dissolution. *ACS Appl. Mater. Interfaces* **2017**, *9*, 21390–21396.

(101) Zhang, J.; Zhou, L.; Du, Q.; Shen, Z.; Hu, J.; Zhang, Y. Assembly of Peptides in Mica-Graphene Nanocapillaries Controlled by Confined Water. *Nanoscale* **2019**, *11*, 8210–8218.

(102) Fan, J. Q.; Li, Y. J.; Wei, Z. J.; Fan, Y.; Li, X. D.; Chen, Z. M.; Hou, D. Y.; Xiao, W. Y.; Ding, M. R.; Wang, H.; Wang, L. Binding-Induced Fibrillogenesis Peptides Recognize and Block Intracellular Vimentin Skeletonization Against Breast Cancer. *Nano Lett.* **2021**, *21*, 6202–6210.

(103) Mang, D.; Roy, S. R.; Zhang, Q.; Hu, X.; Zhang, Y. Heparan Sulfate-Instructed Self-Assembly Selectively Inhibits Cancer Cell Migration. *ACS Appl. Mater. Interfaces* **2021**, *13*, 17236–17242.

(104) Zhang, L.; Jing, D.; Jiang, N.; Rojalin, T.; Baehr, C. M.; Zhang, D.; Xiao, W.; Wu, Y.; Cong, Z.; Li, J. J.; Li, Y.; Wang, L.; Lam, K. S. Transformable Peptide Nanoparticles Arrest HER2 Signalling and Cause Cancer Cell Death *in vivo*. *Nat. Nanotechnol.* **2020**, *15*, 145–153.

(105) Yan, J.; Wang, Y.; Li, X.; Guo, D.; Zhou, Z.; Bai, G.; Li, J.; Huang, N.; Diao, J.; Li, Y.; He, W.; Liu, W.; Tao, K. A Bionic Nano-Band-Aid Constructed by the Three-Stage Self-Assembly of Peptides for Rapid Liver Hemostasis. *Nano Lett.* **2021**, *21*, 7166–7174.

(106) Tao, M.; Xu, K.; He, S.; Li, H.; Zhang, L.; Luo, X.; Zhong, W. Zinc-Ion-Mediated Self-Assembly of Forky Peptides for Prostate Cancer-Specific Drug Delivery. *Chem. Commun. (Camb.)* **2018**, *54*, 4673–4676.

(107) Zhao, X.; Pan, F.; Xu, H.; Yaseen, M.; Shan, H.; Hauser, C. A.; Zhang, S.; Lu, J. R. Molecular Self-Assembly and Applications of Designer Peptide Amphiphiles. *Chem. Soc. Rev.* **2010**, *39*, 3480–98.

(108) Muttenthaler, M.; King, G. F.; Adams, D. J.; Alewood, P. F. Trends in Peptide Drug Discovery. *Nat. Rev. Drug. Discovery* **2021**, *20*, 309–325.

(109) Dai, J.; Hu, J. J.; Dong, X.; Chen, B.; Dong, X.; Liu, R.; Xia, F.; Lou, X. Deep Downregulation of PD-L1 by Caged Peptide-Conjugated AIEgen/miR-140 Nanoparticles for Enhanced Immunotherapy. *Angew. Chem., Int. Ed. Engl.* **2022**, *61*, No. e202117798.

(110) Sun, Y.; Lyu, B.; Yang, C.; He, B.; Zhang, H.; Wang, X.; Zhang, Q.; Dai, W. An Enzyme-Responsive and Transformable PD-L1 Blocking Peptide-Photosensitizer Conjugate Enables Efficient Photothermal Immunotherapy for Breast Cancer. *Bioact. Mater.* **2023**, *22*, 47–59.

(111) Kumar, S.; Bajaj, A. Advances in Self-Assembled Injectable Hydrogels for Cancer Therapy. *Biomater. Sci.* **2020**, *8*, 2055–2073.

(112) Yu, X.; Dai, Y.; Zhao, Y.; Qi, S.; Liu, L.; Lu, L.; Luo, Q.; Zhang, Z. Melittin-Lipid Nanoparticles Target to Lymph Nodes and Elicit a Systemic Anti-Tumor Immune Response. *Nat. Commun.* **2020**, *11*, 1110.

(113) Su, T.; Cheng, F.; Qi, J.; Zhang, Y.; Zhou, S.; Mei, L.; Fu, S.; Zhang, F.; Lin, S.; Zhu, G. Responsive Multivesicular Polymeric Nanovaccines that Codeliver STING Agonists and Neoantigens for Combination Tumor Immunotherapy. *Adv. Sci.* **2022**, *9*, No. e2201895.

(114) Eskandari, S.; Guerin, T.; Toth, I.; Stephenson, R. J. Recent Advances in Self-Assembled Peptides: Implications for Targeted Drug Delivery and Vaccine Engineering. *Adv. Drug Delivery Rev.* **2017**, *110–111*, 169–187.

(115) Chen, J.; Zou, X. Self-Assemble Peptide Biomaterials and Their Biomedical Applications. *Bioact. Mater.* **2019**, *4*, 120–131.

(116) Cao, M.; Lu, S.; Wang, N.; Xu, H.; Cox, H.; Li, R.; Waigh, T.; Han, Y.; Wang, Y.; Lu, J. R. Enzyme-Triggered Morphological Transition of Peptide Nanostructures for Tumor-Targeted Drug Delivery and Enhanced Cancer Therapy. *ACS Appl. Mater. Interfaces* **2019**, *11*, 16357–16366.

(117) Tang, J.; Zeng, Z.; Yan, J.; Chen, C.; Liu, J.; Feng, X. Quantitative and High Drug Loading of Self-Assembled Prodrug with Defined Molecular Structures for Effective Cancer Therapy. *J. Controlled Release* **2019**, *307*, 90–97.

(118) Zhu, Y.; Wang, L.; Li, Y.; Huang, Z.; Luo, S.; He, Y.; Han, H.; Raza, F.; Wu, J.; Ge, L. Injectable pH and Redox Dual Responsive Hydrogels Based on Self-Assembled Peptides for Anti-Tumor Drug Delivery. *Biomater. Sci.* **2020**, *8*, 5415–5426.

(119) Jiang, X.; Fan, X.; Xu, W.; Zhao, C.; Wu, H.; Zhang, R.; Wu, G. Self-Assembled Peptide Nanoparticles Responsive to Multiple Tumor Microenvironment Triggers Provide Highly Efficient Targeted Delivery and Release of Antitumor Drug. *J. Controlled Release* **2019**, *316*, 196–207.

(120) Sun, Y.; Liu, L.; Zhou, L.; Yu, S.; Lan, Y.; Liang, Q.; Liu, J.; Cao, A.; Liu, Y. Tumor Microenvironment-Triggered Charge Reversal Polymetformin-Based Nanosystem Co-Delivered Doxorubicin and IL-12 Cytokine Gene for Chemo-Gene Combination Therapy on Metastatic Breast Cancer. *ACS Appl. Mater. Interfaces* **2020**, *12*, 45873–45890.

(121) Liu, S.; Zhang, Y.; Zhao, X.; Wang, J.; Di, C.; Zhao, Y.; Ji, T.; Cheng, K.; Wang, Y.; Chen, L.; Qi, Y.; Li, S.; Nie, G. Tumor-Specific Silencing of Tissue Factor Suppresses Metastasis and Prevents Cancer-Associated Hypercoagulability. *Nano Lett.* **2019**, *19*, 4721–4730.

(122) Lin, Y. X.; Wang, Y.; An, H. W.; Qi, B.; Wang, J.; Wang, L.; Shi, J.; Mei, L.; Wang, H. Peptide-Based Autophagic Gene and Cisplatin Co-Delivery Systems Enable Improved Chemotherapy Resistance. *Nano Lett.* **2019**, *19*, 2968–2978.

(123) Jiang, L.; Chen, D.; Jin, Z.; Xia, C.; Xu, Q.; Fan, M.; Dai, Y.; Liu, J.; Li, Y.; He, Q. Light-Triggered Nitric Oxide Release and Structure Transformation of Peptide for Enhanced Intratumoral Retention and Sensitized Photodynamic Therapy. *Bioact. Mater.* **2022**, *12*, 303–313.

(124) Guo, R. C.; Zhang, X. H.; Ji, L.; Wei, Z. J.; Duan, Z. Y.; Qiao, Z. Y.; Wang, H. Recent Progress of Therapeutic Peptide Based Nanomaterials: From Synthesis and Self-Assembly to Cancer Treatment. *Biomater. Sci.* **2020**, *8*, 6175–6189.

(125) Chen, S.; Fan, J. X.; Liu, X. H.; Zhang, M. K.; Liu, F.; Zeng, X.; Yan, G. P.; Zhang, X. Z. A self-Delivery System Based on an Amphiphilic Proapoptotic Peptide for Tumor Targeting Therapy. *J. Mater. Chem. B* **2019**, *7*, 778–785.

(126) Sarangthem, V.; Yi, A.; Kim, Y.; Rehemtulla, A.; Lee, B. H.; Jeon, Y. H.; Singh, T. D.; Park, R. W. Therapeutic Effect of IL-4 Receptor-Targeting Pro-Apoptotic Peptide (AP1-ELP-KLAK) in Glioblastoma Tumor Model. *Int. J. Nanomed.* **2021**, *16*, 5039–5052.

(127) Jia, H. R.; Zhu, Y. X.; Liu, X.; Pan, G. Y.; Gao, G.; Sun, W.; Zhang, X.; Jiang, Y. W.; Wu, F. G. Construction of Dually Responsive Nanotransformers with Nanosphere-Nanofiber-Nanosphere Transition for Overcoming the Size Paradox of Anticancer Nanodrugs. *ACS Nano* **2019**, *13*, 11781–11792.

(128) Jung, H. K.; Kim, S.; Park, R. W.; Park, J. Y.; Kim, I. S.; Lee, B. Bladder Tumor-Targeted Delivery of Pro-Apoptotic Peptide for Cancer Therapy. *J. Controlled Release* **2016**, *235*, 259–267.

(129) Tang, Y.; Wu, Z.; Zhang, C. H.; Zhang, X. L.; Jiang, J. H. Enzymatic Activatable Self-Assembled Peptide Nanowire for Targeted Therapy and Fluorescence Imaging of Tumors. *Chem. Commun. (Camb.)* **2016**, *52*, 3631–4.

(130) Ding, Y.; Ji, T.; Zhao, Y.; Zhang, Y.; Zhao, X.; Zhao, R.; Lang, J.; Zhao, X.; Shi, J.; Sukumar, S.; Nie, G. Improvement of Stability and Efficacy of C16Y Therapeutic Peptide via Molecular Self-Assembly into Tumor-Responsive Nanoformulation. *Mol. Cancer Ther.* **2015**, *14*, 2390–400.

(131) Chen, B.; Dong, X.; Dong, X.; Wang, Q.; Wu, M.; Wu, J.; Lou, X.; Xia, F.; Wang, W.; Dai, J.; Wang, S. Integration of Dual Targeting and Dual Therapeutic Modules Endows Self-Assembled Nanoparticles with Anti-Tumor Growth and Metastasis Functions. *Int. J. Nanomed.* **2021**, *16*, 1361–1376.

(132) Dai, X.; Meng, J.; Deng, S.; Zhang, L.; Wan, C.; Lu, L.; Huang, J.; Hu, Y.; Zhang, Z.; Li, Y.; Lovell, J. F.; Wu, G.; Yang, K.; Jin, H. Targeting CAMKII to Reprogram Tumor-Associated Macrophages and Inhibit Tumor Cells for Cancer Immunotherapy with an Injectable Hybrid Peptide Hydrogel. *Theranostics* **2020**, *10*, 3049–3063.

(133) Jia, W.; Liu, R.; Wang, Y.; Hu, C.; Yu, W.; Zhou, Y.; Wang, L.; Zhang, M.; Gao, H.; Gao, X. Dual-Responsive Nanoparticles with Transformable Shape and Reversible Charge for Amplified Chemo-Photodynamic Therapy of Breast Cancer. *Acta Pharm. Sin. B* **2022**, *12*, 3354–3366.

(134) Ji, Y.; Xiao, Y.; Xu, L.; He, J.; Qian, C.; Li, W.; Wu, L.; Chen, R.; Wang, J.; Hu, R.; Zhang, X.; Gu, Z.; Chen, Z. Drug-Bearing Supramolecular MMP Inhibitor Nanofibers for Inhibition of Metastasis and Growth of Liver Cancer. *Adv. Sci. (Weinh.)* **2018**, *5*, 1700867.

(135) Baehr, C. M.; Zhang, L.; Wu, Y.; Domokos, A.; Xiao, W.; Wang, L.; Lam, K. S. Transformable Amyloid-Beta Mimetic Peptide Amphiphiles for Lysosomal Disruption in Non-Small Cell Lung Cancer. *Biomaterials* **2021**, *277*, 121078.

(136) Luo, S.; Feng, J.; Xiao, L.; Guo, L.; Deng, L.; Du, Z.; Xue, Y.; Song, X.; Sun, X.; Zhang, Z.; Fu, Y.; Gong, T. Targeting Self-Assembly Peptide for Inhibiting Breast Tumor Progression and Metastasis. *Biomaterials* **2020**, *249*, 120055.

(137) Wang, T.; He, Z.; Yuan, C.-S.; Deng, Z.-W.; Li, F.; Chen, X.-G.; Liu, Y. MMP-Responsive Transformation Nanomaterials with IAP Antagonist to Boost Immune Checkpoint Therapy. *J. Controlled Release* **2022**, *343*, 765–776.

(138) Brezden, A.; Mohamed, M. F.; Nepal, M.; Harwood, J. S.; Kuriakose, J.; Seleem, M. N.; Chmielewski, J. Dual Targeting of Intracellular Pathogenic Bacteria with a Cleavable Conjugate of Kanamycin and an Antibacterial Cell-Penetrating Peptide. *J. Am. Chem. Soc.* **2016**, *138*, 10945–9.

(139) Zou, P.; Chen, W. T.; Sun, T.; Gao, Y.; Li, L. L.; Wang, H. Recent Advances: Peptides and Self-Assembled Peptide-Nanosystems for Antimicrobial Therapy and Diagnosis. *Biomater. Sci.* **2020**, *8*, 4975–4996.

(140) Huang, R.; Yu, Q. H.; Yao, X. D.; Liu, W. L.; Cheng, Y. J.; Ma, Y. H.; Zhang, A. Q.; Qin, S. Y. Self-Deliverable Peptide-Mediated and Reactive-Oxygen-Species-Amplified Therapeutic Nanoplatform for Highly Effective Bacterial Inhibition. *ACS Appl. Mater. Interfaces* **2022**, *14*, 159–171.

(141) Lombardi, L.; Falanga, A.; Del Genio, V.; Galdiero, S. A New Hope: Self-Assembling Peptides with Antimicrobial Activity. *Pharmaceutics* **2019**, *11*, 166.

(142) Zhang, Q. Y.; Yan, Z. B.; Meng, Y. M.; Hong, X. Y.; Shao, G.; Ma, J. J.; Cheng, X. R.; Liu, J.; Kang, J.; Fu, C. Y. Antimicrobial Peptides: Mechanism of Action, Activity and Clinical Potential. *Mil. Med. Res.* **2021**, *8*, 48.

(143) Yu, Q. H.; Huang, R.; Wu, K. Y.; Han, X. L.; Cheng, Y. J.; Liu, W. L.; Zhang, A. Q.; Qin, S. Y. Infection-Activated Lipopeptide Nanotherapeutics with Adaptable Geometrical Morphology for *in vivo* Bacterial Ablation. *Acta Biomater.* **2022**, *154*, 359–373.

(144) Pranantyo, D.; Kang, E. T.; Chan-Park, M. B. Smart Nanomicelles with Bacterial Infection-Responsive Disassembly for Selective Antimicrobial Applications. *Biomater. Sci.* **2021**, *9*, 1627–1638.

(145) Li, L.; Gu, P.; Hao, M.; Xiang, X.; Feng, Y.; Zhu, X.; Song, Y.; Song, E. Bacteria-Targeted MRI Probe-Based Imaging Bacterial Infection and Monitoring Antimicrobial Therapy *in vivo*. *Small* **2021**, *17*, No. e2103627.

(146) Qi, G. B.; Zhang, D.; Liu, F. H.; Qiao, Z. Y.; Wang, H. An “On-Site Transformation” Strategy for Treatment of Bacterial Infection. *Adv. Mater.* **2017**, *29*, 1703461.

(147) Fan, Y.; Li, X. D.; He, P. P.; Hu, X. X.; Zhang, K.; Fan, J. Q.; Yang, P. P.; Zheng, H. Y.; Tian, W.; Chen, Z. M.; Ji, L.; Wang, H.; Wang, L. A Biomimetic Peptide Recognizes and Traps Bacteria *in vivo* as Human Defensin-6. *Sci. Adv.* **2020**, *6*, No. eaaz4767.

(148) Wang, Y.; Li, X.; Yuan, J.; Wang, X.; Tao, K.; Yan, J. A Bionic Self-Assembly Hydrogel Constructed by Peptides with Favorable Biosecurity, Rapid Hemostasis and Antibacterial Property for Wound Healing. *Front. Bioeng. Biotechnol.* **2022**, *10*, 901534.

(149) Zhou, Y.; Liu, S.; Zhao, M.; Wang, C.; Li, L.; Yuan, Y.; Li, L.; Liao, G.; Bresette, W.; Zhang, J.; Chen, Y.; Cheng, J.; Lu, Y.; Liu, J. Injectable Extracellular Vesicle-Released Self-Assembling Peptide Nanofiber Hydrogel as an Enhanced Cell-Free Therapy for Tissue Regeneration. *J. Controlled Release* **2019**, *316*, 93–104.

(150) Guan, T.; Li, J.; Chen, C.; Liu, Y. Self-Assembling Peptide-Based Hydrogels for Wound Tissue Repair. *Adv. Sci.* **2022**, *9*, No. e2104165.

(151) Zhang, M.; Li, L.; An, H.; Zhang, P.; Liu, P. Repair of Peripheral Nerve Injury Using Hydrogels Based on Self-Assembled Peptides. *Gels* **2021**, *7*, 152.

(152) Yadav, N.; Chauhan, M. K.; Chauhan, V. S. Short to Ultrashort Peptide-Based Hydrogels as a Platform for Biomedical Applications. *Biomater. Sci.* **2020**, *8*, 84–100.

(153) Poongodi, R.; Chen, Y. L.; Yang, T. H.; Huang, Y. H.; Yang, K. D.; Lin, H. C.; Cheng, J. K. Bio-Scaffolds as Cell or Exosome Carriers for Nerve Injury Repair. *Int. J. Mol. Sci.* **2021**, *22*, 13347.

(154) Koss, K. M.; Unsworth, L. D. Neural Tissue Engineering: Bioresponsive Nanoscaffolds Using Engineered Self-Assembling Peptides. *Acta Biomater.* **2016**, *44*, 2–15.

(155) Rizzo, M. G.; Palermo, N.; D'Amora, U.; Oddo, S.; Guglielmino, S. P. P.; Conoci, S.; Szychlinska, M. A.; Calabrese, G. Multipotential Role of Growth Factor Mimetic Peptides for Osteochondral Tissue Engineering. *Int. J. Mol. Sci.* **2022**, *23*, 7388.

(156) Lu, J.; Wang, X. Biomimetic Self-Assembling Peptide Hydrogels for Tissue Engineering Applications. *Adv. Exp. Med. Biol.* **2018**, *1064*, 297–312.

(157) Sawicka, J.; Ilowska, E.; Deptula, M.; Sosnowski, P.; Sass, P.; Czerwic, K.; Chmielewska, K.; Szymanska, A.; Pietralik-Molinska, Z.; Kozak, M.; Sachadyn, P.; Pikula, M.; Rodziewicz-Motowidlo, S. Functionalized Peptide Fibrils as a Scaffold for Active Substances in Wound Healing. *Int. J. Mol. Sci.* **2021**, *22*, 3818.

(158) Liu, S.; Zhao, M.; Zhou, Y.; Li, L.; Wang, C.; Yuan, Y.; Li, L.; Liao, G.; Bresette, W.; Chen, Y.; Cheng, J.; Lu, Y.; Liu, J. A Self-Assembling Peptide Hydrogel-Based Drug Co-Delivery Platform to Improve Tissue Repair After Ischemia-Reperfusion Injury. *Acta Biomater.* **2020**, *103*, 102–114.

(159) Vong, L. B.; Ibayashi, Y.; Lee, Y.; Ngo, D. N.; Nishikawa, Y.; Nagasaki, Y. Poly(Lornithine)-Based Self-Assembling Drug for Recovery of Hyperammonemia and Damage in Acute Liver Injury. *J. Controlled Release* **2019**, *310*, 74–81.

(160) Guan, S.; Munder, A.; Hedtfeld, S.; Braubach, P.; Glage, S.; Zhang, L.; Lienenklaus, S.; Schultze, A.; Hasenpusch, G.; Garrels, W.; Stanke, F.; Miskey, C.; Johler, S. M.; Kumar, Y.; Tummler, B.; Rudolph, C.; Ivics, Z.; Rosenacker, J. Self-Assembled Peptide-Poloxamine Nanoparticles Enable *in vitro* and *in vivo* Genome Restoration for Cystic Fibrosis. *Nat. Nanotechnol.* **2019**, *14*, 287–297.

(161) Nguyen, M. M.; Carlini, A. S.; Chien, M. P.; Sonnenberg, S.; Luo, C.; Braden, R. L.; Osborn, K. G.; Li, Y.; Gianneschi, N. C.; Christman, K. L. Enzyme-Responsive Nanoparticles for Targeted Accumulation and Prolonged Retention in Heart Tissue After Myocardial Infarction. *Adv. Mater.* **2015**, *27*, 5547–52.

(162) Hu, Y.; Wang, Y.; Deng, J.; Ding, X.; Lin, D.; Shi, H.; Chen, L.; Lin, D.; Wang, Y.; Vakal, S.; Wang, J.; Li, X. Enzyme-Instructed Self-Assembly of Peptide-Drug Conjugates in Tear Fluids for Ocular Drug Delivery. *J. Controlled Release* **2022**, *344*, 261–271.

(163) Yu, X.; Zhang, Z.; Yu, J.; Chen, H.; Li, X. Self-Assembly of a Ibuprofen-Peptide Conjugate to Suppress Ocular Inflammation. *Nanomedicine* **2018**, *14*, 185–193.

(164) Chen, H.; Shou, K.; Chen, S.; Qu, C.; Wang, Z.; Jiang, L.; Zhu, M.; Ding, B.; Qian, K.; Ji, A.; Lou, H.; Tong, L.; Hsu, A.; Wang, Y.; Felsher, D. W.; Hu, Z.; Tian, J.; Cheng, Z. Smart Self-Assembly Amphiphilic Cyclopeptide-Dye for Near-Infrared Window-II Imaging. *Adv. Mater.* **2021**, *33*, No. e2006902.

(165) Guo, M.; Zhang, L.; Tian, Y.; Wang, M.; Wang, W. Living-System-Driven Evolution of Self-Assembled-Peptide Probes: for Boosting Glioma Theranostics. *Anal. Chem.* **2021**, *93*, 8035–8044.

(166) Zheng, R.; Yang, J.; Mamuti, M.; Hou, D. Y.; An, H. W.; Zhao, Y.; Wang, H. Controllable Self-Assembly of Peptide-Cyanine Conjugates *in vivo* as Fine-Tunable Theranostics. *Angew. Chem., Int. Ed. Engl.* **2021**, *60*, 7809–7819.

(167) Lu, S.; Guo, X.; Zhang, F.; Li, X.; Zou, M.; Li, L.-L. Bioactivated *in vivo* Assembly (BIVA) Peptide-Tetraphenylethylene (TPE) Probe with Controllable Assembled Nanostructure for Cell Imaging. *Chin. Chem. Lett.* **2021**, *32*, 1947–1952.

(168) Gao, J.; Li, J.; Wei, D.; Yang, H.; Duan, Y.; Zhang, Y.; Gong, X.; Wang, H.; Ding, D.; Wu, X.; Chang, J. Enabling AIgens Close Assembly in Tumor-Overexpressed Protein Cluster for Boosted Image-Guided Cancer Surgery. *Sci. China: Chem.* **2020**, *63*, 1694–1702.

(169) Zhang, X.; Ren, C.; Hu, F.; Gao, Y.; Wang, Z.; Li, H.; Liu, J.; Liu, B.; Yang, C. Detection of Bacterial Alkaline Phosphatase Activity by Enzymatic *in situ* Self-Assembly of the AIEgen-Peptide Conjugate. *Anal. Chem.* **2020**, *92*, 5185–5190.

(170) Wang, D.; Cheng, D. B.; Ji, L.; Niu, L. J.; Zhang, X. H.; Cong, Y.; Cao, R. H.; Zhou, L.; Bai, F.; Qiao, Z. Y.; Wang, H. Precise Magnetic Resonance Imaging-Guided Sonodynamic Therapy for Drug-Resistant Bacterial Deep Infection. *Biomaterials* **2021**, *264*, 120386.

(171) Gallo, E.; Diaferia, C.; Di Gregorio, E.; Morelli, G.; Gianolio, E.; Accardo, A. Peptide-Based Soft Hydrogels Modified with Gadolinium Complexes as MRI Contrast Agents. *Pharmaceutics (Basel)* **2020**, *13*, 19.

(172) Gu, L.; Li, X.; Jiang, J.; Guo, G.; Wu, H.; Wu, M.; Zhu, H. Stem Cell Tracking Using Effective Self-Assembled Peptide-Modified Superparamagnetic Nanoparticles. *Nanoscale* **2018**, *10*, 15967–15979.

(173) Ji, Y.; Jones, C.; Baek, Y.; Park, G. K.; Kashiwagi, S.; Choi, H. S. Near-Infrared Fluorescence Imaging in Immunotherapy. *Adv. Drug Delivery Rev.* **2020**, *167*, 121–134.

(174) Ren, C.; Wang, Z.; Zhang, X.; Gao, J.; Gao, Y.; Zhang, Y.; Liu, J.; Yang, C.; Liu, J. Construction of All-in-One Peptide Nanomedicine with Photoacoustic Imaging Guided Mild Hyperthermia for Enhanced Cancer Chemotherapy. *Chem. Eng. J.* **2021**, *405*, 127008.

(175) Xia, X.; Wang, X.; Han, X.; Qi, M.; Gao, Y.; Liao, J.; He, X.; Pan, K.; Cheng, Q.; Wang, Q. Construction of Self-Assembled Nanogel as Multienzyme Mimics for Bioresponsive Tandem-Catalysis Imaging. *Sci. China Mater.* **2021**, *64*, 3079–3086.

(176) Rizvi, S. F. A.; Shahid, S.; Mu, S.; Zhang, H. Hybridization of Tumor Homing and Mitochondria-Targeting Peptide Domains to Design Novel Dual-Imaging Self-Assembled Peptide Nanoparticles for Theranostic Applications. *Drug Delivery Transl. Res.* **2022**, *12*, 1774–1785.

(177) Lin, L.; Xie, Z.; Xu, M.; Wang, Y.; Li, S.; Yang, N.; Gong, X.; Liang, P.; Zhang, X.; Song, L.; Cao, F. IVUS\IVPA Hybrid Intravascular Molecular Imaging of Angiogenesis in Atherosclerotic Plaques via RGDfk Peptide-Targeted Nanoprobes. *Photoacoustics* **2021**, *22*, 100262.

(178) Gelain, F.; Luo, Z.; Rioult, M.; Zhang, S. Self-Assembling Peptide Scaffolds in the Clinic. *NPJ. Regen. Med.* **2021**, *6*, 9.

(179) Sankar, S.; O'Neill, K.; Bagot D'Arc, M.; Rebeca, F.; Buffier, M.; Aleksi, E.; Fan, M.; Matsuda, N.; Gil, E. S.; Spirio, L. Clinical Use of the Self-Assembling Peptide RADA16: a Review of Current and Future Trends in Biomedicine. *Front. Bioeng. Biotechnol.* **2021**, *9*, 679525.

(180) Carratala, J. V.; Serna, N.; Villaverde, A.; Vazquez, E.; Ferrer-Miralles, N. Nanostructured Antimicrobial Peptides: the Last Push Towards Clinics. *Biotechnol. Adv.* **2020**, *44*, 107603.

(181) Han, C.; Zhang, Z.; Sun, J.; Li, K.; Li, Y.; Ren, C.; Meng, Q.; Yang, J. Self-Assembling Peptide-Based Hydrogels in Angiogenesis. *Int. J. Nanomed.* **2020**, *15*, 10257–10269.